

An intercomparison of CCN and size distribution among AeroCom models. Plans for the aerosol microphysics working group

Graham Mann (NCAS-climate, University of Leeds)

Ken Carslaw, Dominick Spracklen, Kirsty Pringle Carly Reddington, Matt Woodhouse, Lindsay Lee (University of Leeds)

**AEROCOM modellers who've submitted all-aerosol-tracer data
The data is on the benchmark observational datasets.**



**National Centre for
Atmospheric Science**

NATURAL ENVIRONMENT RESEARCH COUNCIL



GLOMAP

Global Model of Aerosol Processes



Aerosol in most climate models

Mass of chemical components (e.g., SO_4 , black carbon, dust) as advected quantities

For size-dependent processes: An assumed size distribution

Direct aerosol forcing: Use composition-dependent mass scattering efficiency (or assume a fixed size distribution)

e.g. for SO_4 , AOD can change only via change in mass.

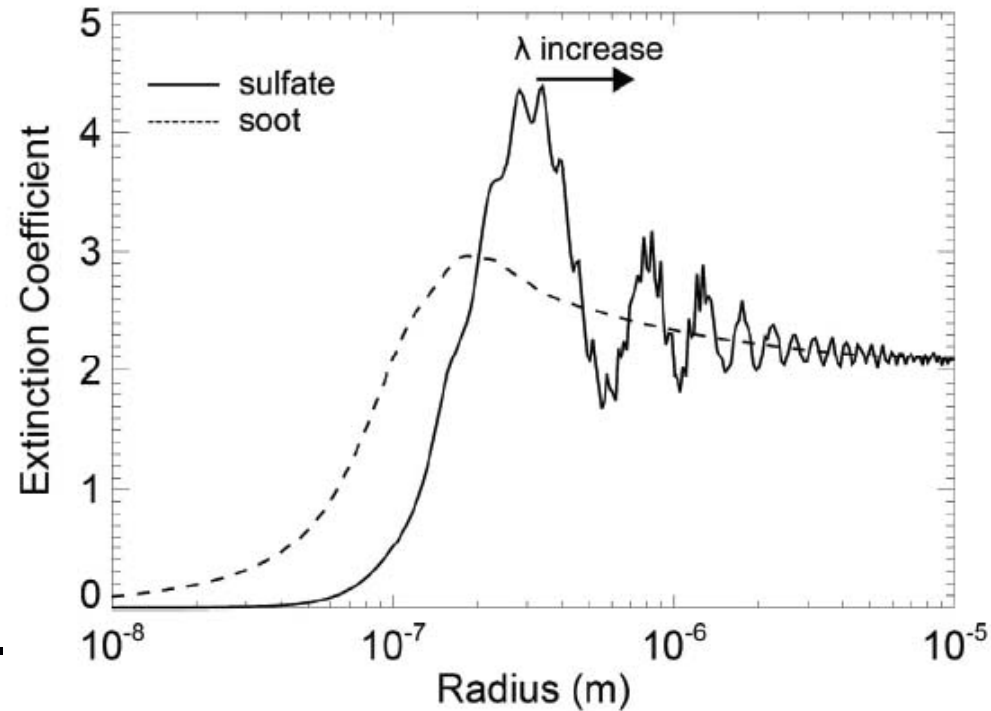
Indirect forcing: Use empirical cloud drop—**aerosol relations**, e.g., Lowenthal et al: $\log(\text{CDN}) = 2.38 + 0.49\log(\text{Mso}_4)$,

--- any change in mass causes increase in CDN.

Importance of size distribution: Aerosol optical depth

Differences in particle size distribution also affect the extinction.

Constant mass extinction efficiency will not capture variability from changes to the particle size distribution.



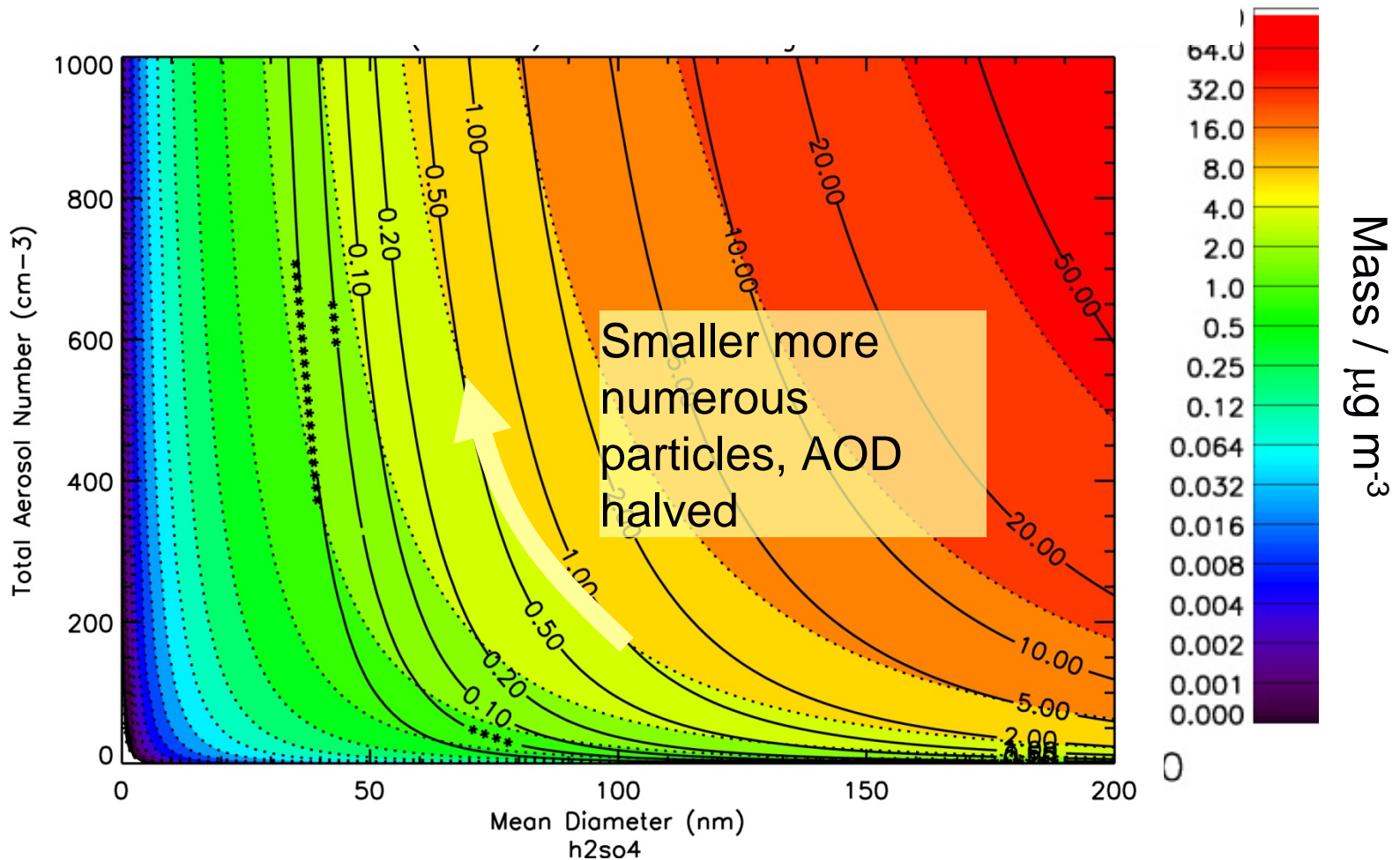
$$b_{ext} = \pi \sum_{i=0}^n Q_{ext} R_i^2 \frac{dN_i}{d \ln R_i} \Delta \ln R_i \quad \tau_{\lambda} = \int_0^{z_{top}} b_{ext}(\lambda) dz ,$$

Changes in size distribution lead to different AOD
Even when the process conserves mass.

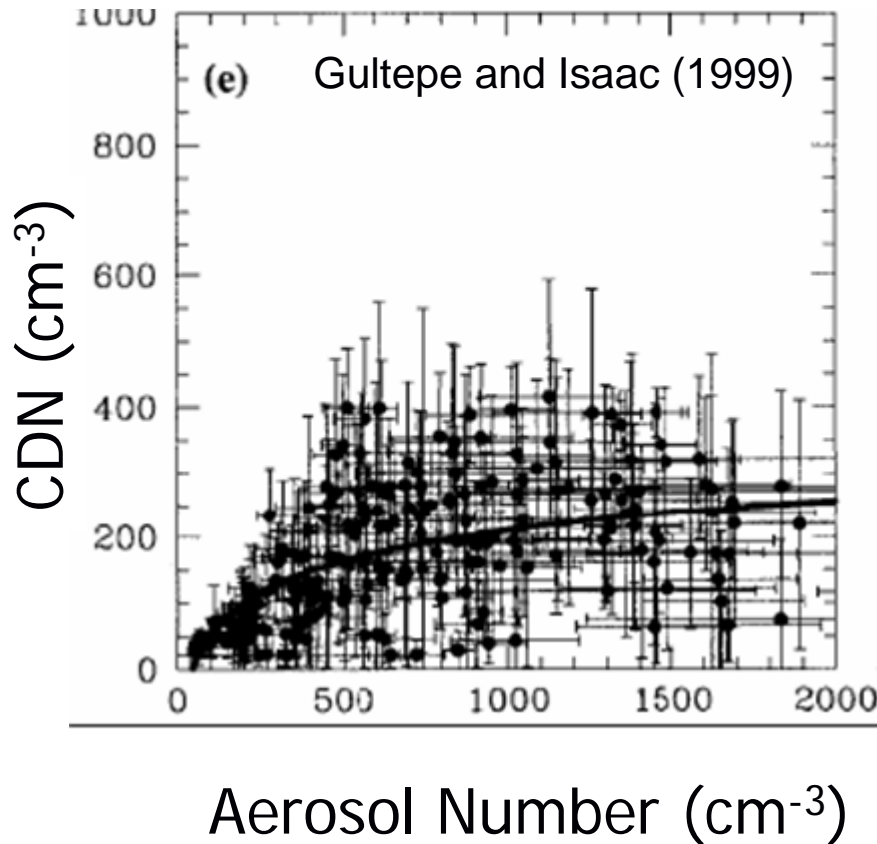


Importance of size distribution: Aerosol optical depth

Mie calculations based on log-normal sulphate aerosol



Calculating CDN in GCMs

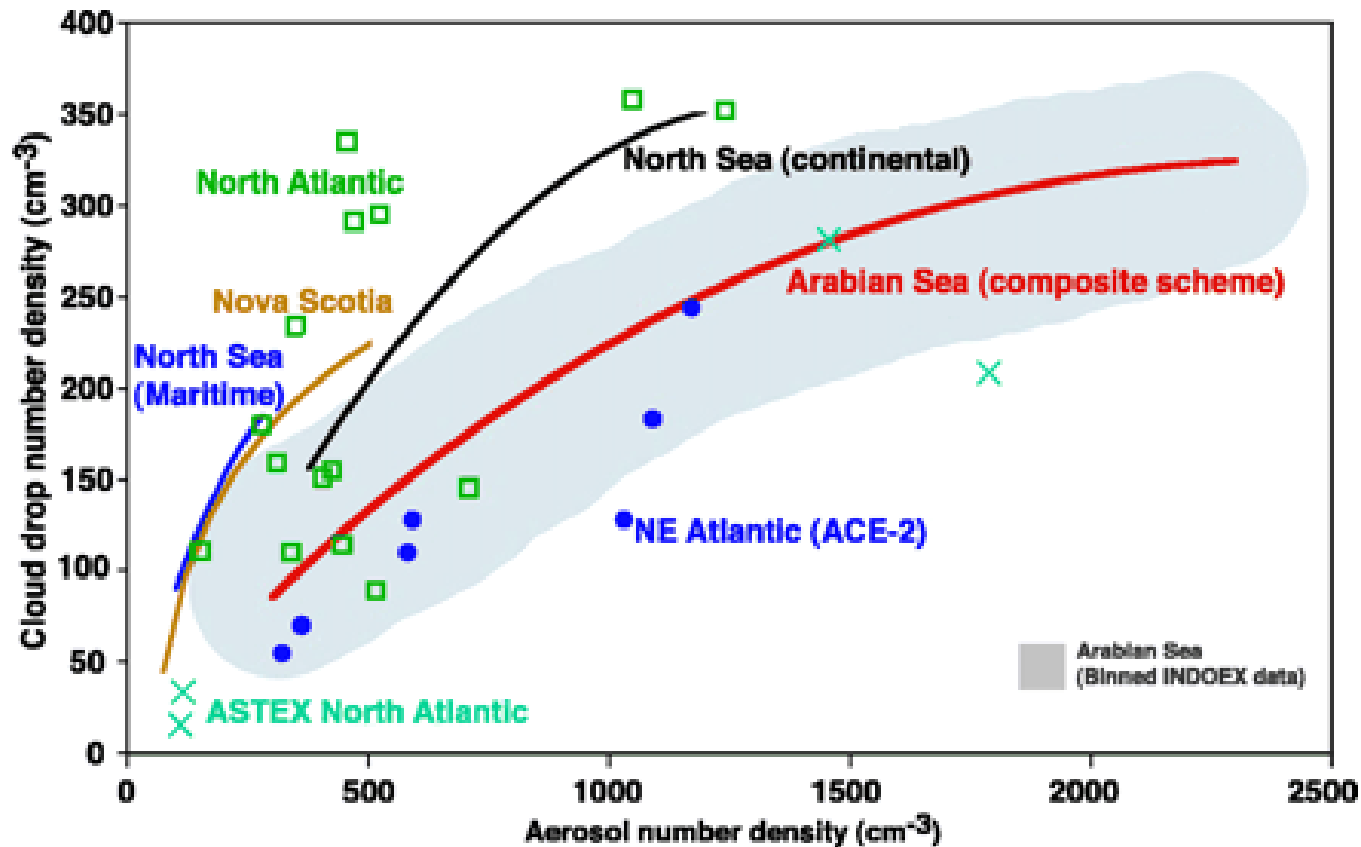


GCM procedure:

1. Measure CDN and aerosol mass (or number) > certain size in same airmass
2. Fit CDN-mass (or number) relation

In mass-only GCM, number is diagnosed not prognosed (i.e., calculated by assuming a size distribution)

Composite of CDN-aerosol observations from many sites



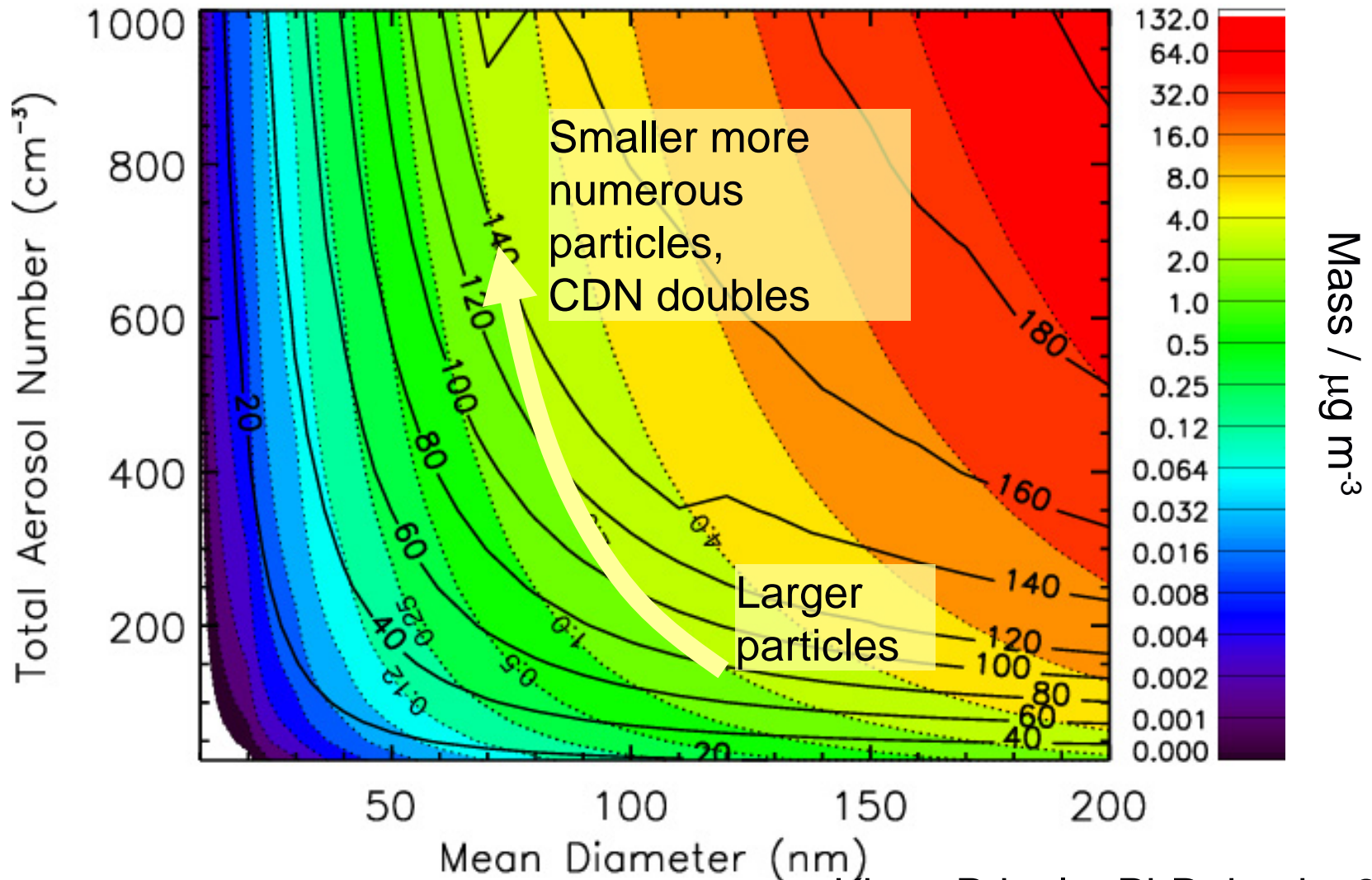
From Ramanathan and Crutzen

No single relationship

Different particle types, compositions, size distributions, etc

Importance of the size distribution: Cloud droplet number \rightarrow indirect effects

Parcel model calculation of cloud drop number from log-normal aerosol



Global Model of Aerosol Processes (GLOMAP)

Global CTM forced by 6-hourly ECMWF winds

Usually run at T42L31 ($2.8^\circ \times 2.8^\circ$) resolution

Sectional aerosol scheme: 20 bins, 3 nm – 20 μm

Modal scheme: 7 or 4 log-normal modes

In TOMCAT CTM usually driven by offline oxidants,
now coupled to tropospheric chemistry

Aerosol transport, new particle formation, growth
by coagulation, condensation, cloud processing.

Wet and dry deposition of gases & aerosol particles

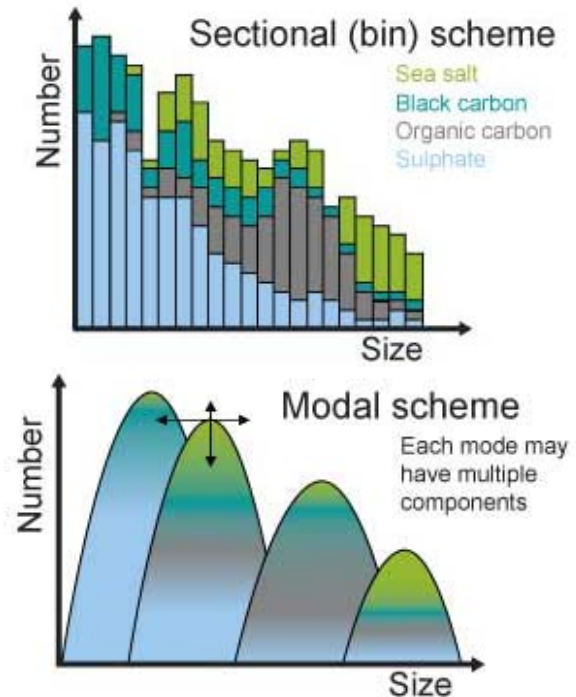
Emissions of $\text{DMS} \rightarrow \text{SO}_2 \rightarrow \text{H}_2\text{SO}_4$; monoterpenes \rightarrow biogenic SOA

Primary emissions of sea salt, dust,
black & organic carbon (fossil and biofuels, vegetation fires)

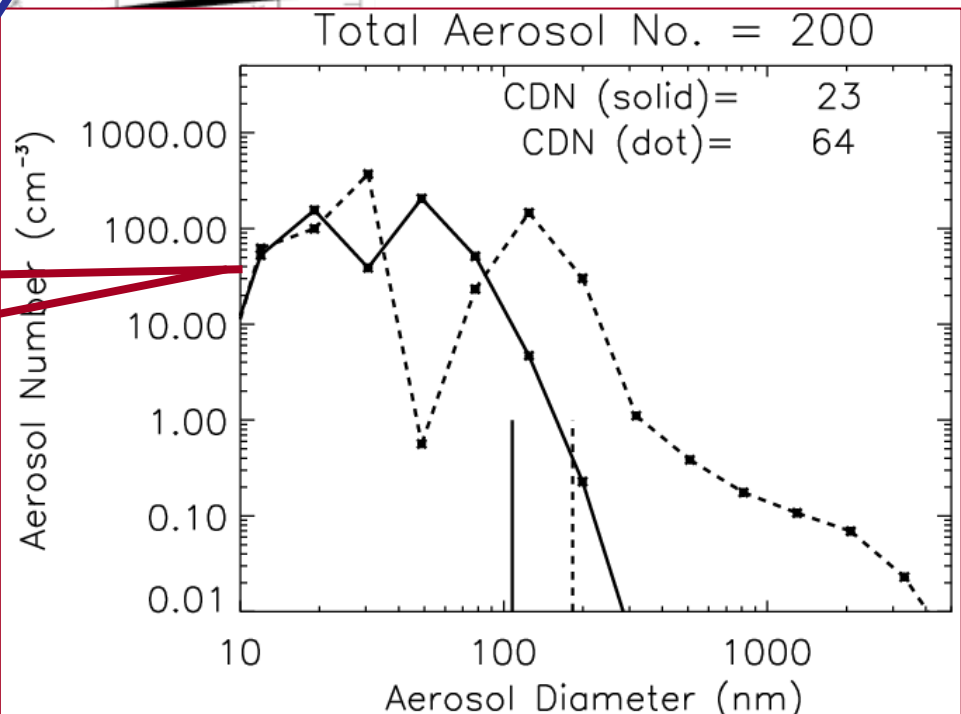
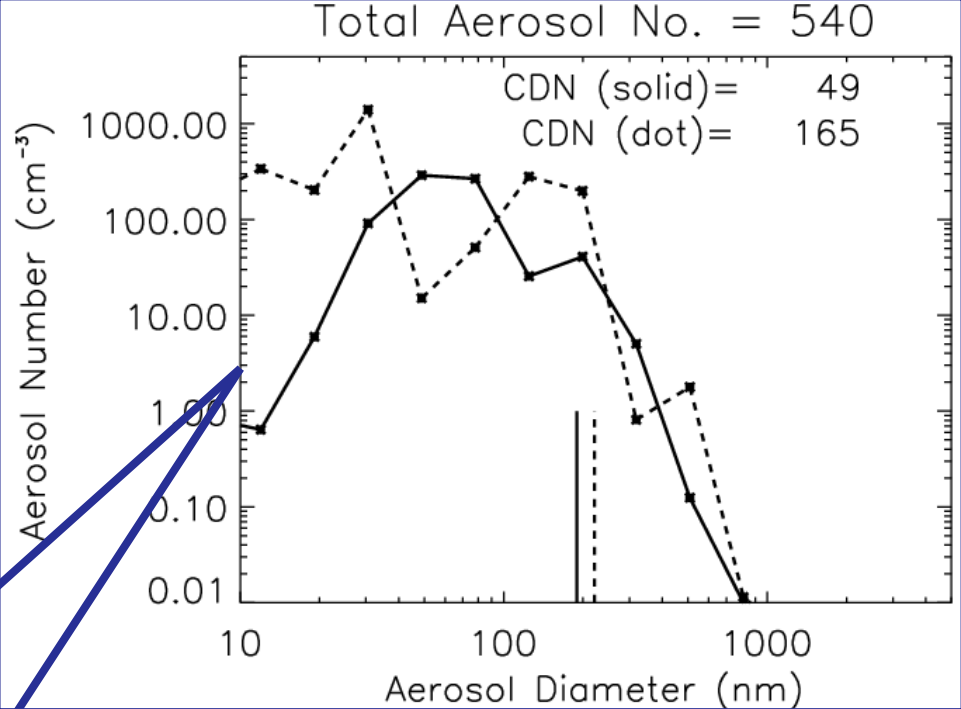
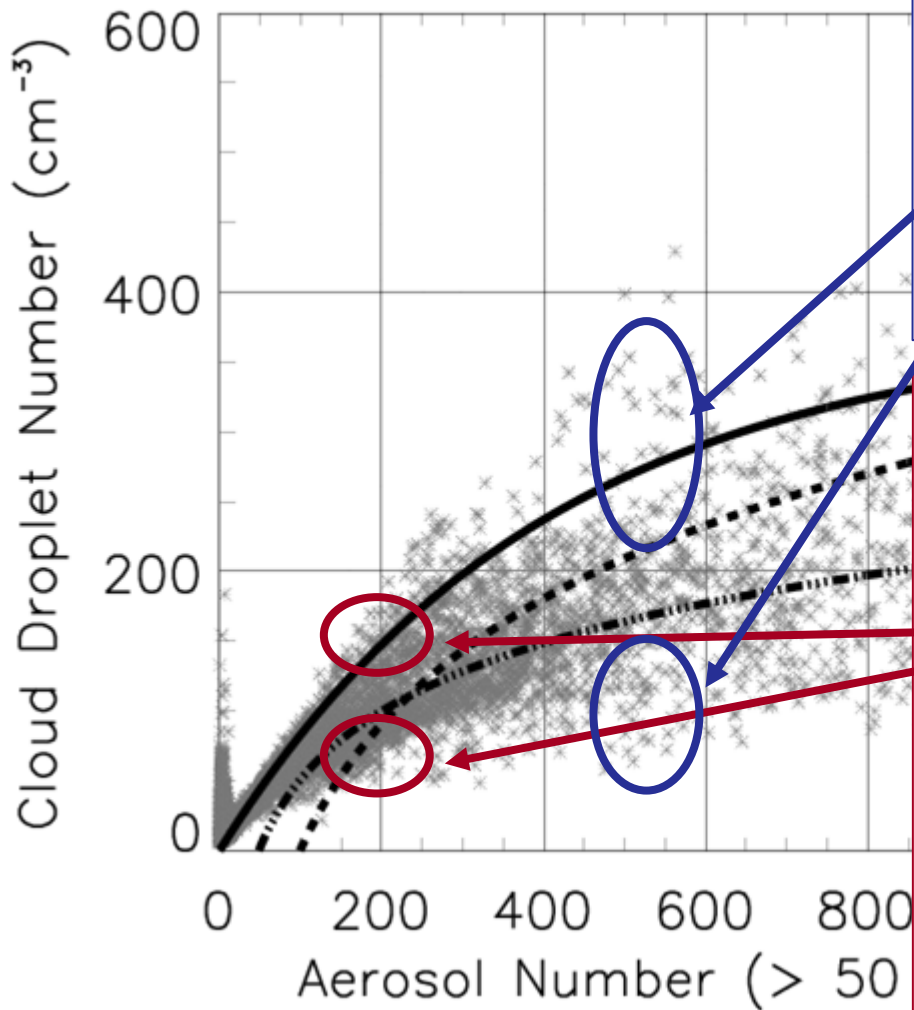
Nucleation via binary homogeneous nucleation of $\text{H}_2\text{SO}_4\text{-H}_2\text{O}$
and also now implemented boundary layer nucleation mechanism

GLOMAP-bin : Spracklen et al. (ACP, 2005), Spracklen et al (GRL, 2008)

GLOMAP-mode: Mann et al (GMD, 2010), Woodhouse et al (2010), Schmidt et al (2010)

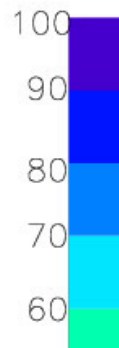
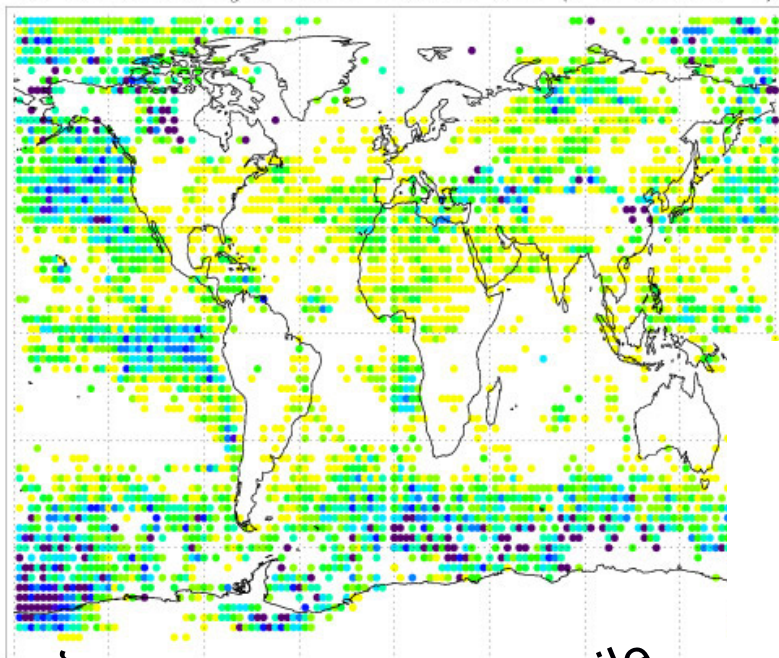


Exploring the scatter in model CDN-aerosol



Variability in predicted CDN

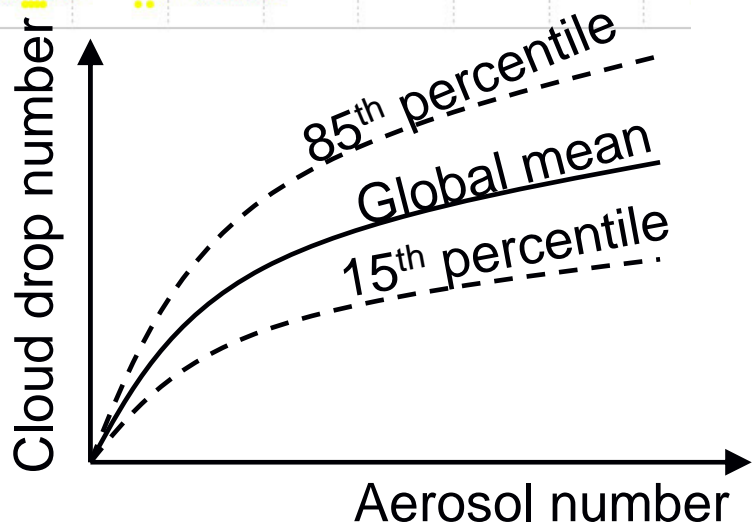
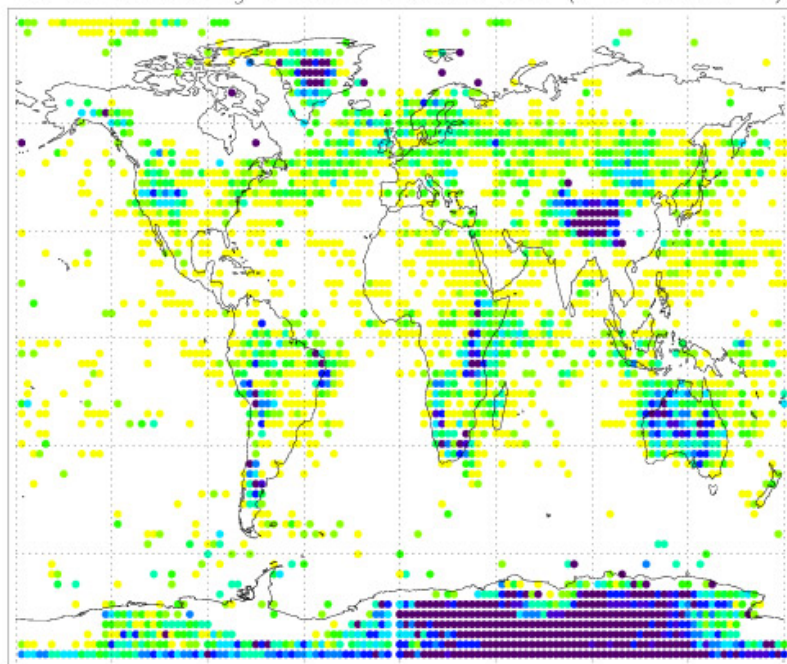
PDF of CDN being $>$ 85th Percentile CDN ($w = 0.15\text{ms}^{-1}$)



Percent of days that exceed 85th percentile

Pringle et al (2009, ACP)

PDF of CDN being $<$ 15th Percentile CDN ($w = 0.15\text{ms}^{-1}$)



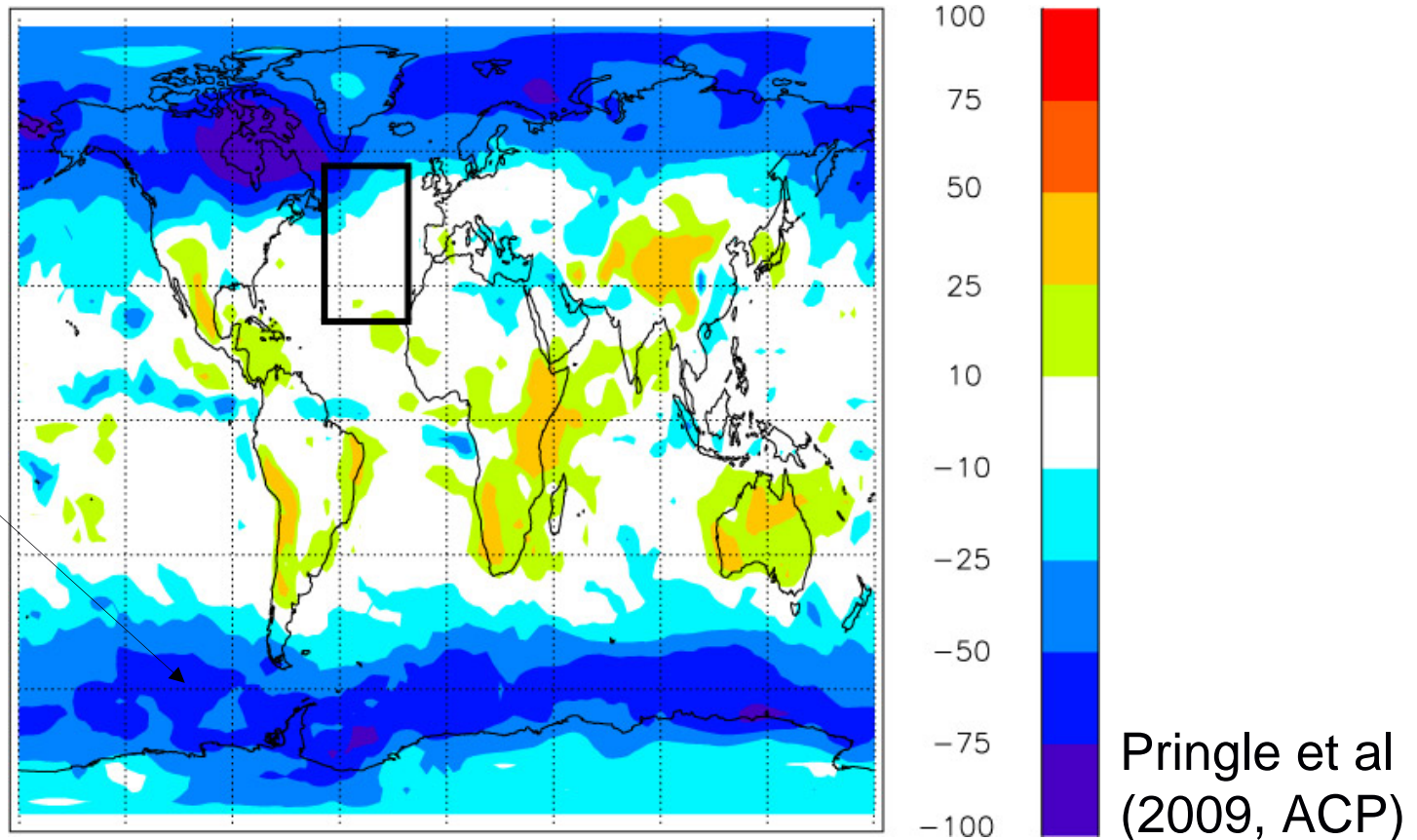
Global CDN prediction based on single-region CDN-aerosol relation

Use model output to generate CDN-aerosol empirical fit

Use the fit to calculate global CDN

Calculate the %difference from mechanistic CDN calculation

75% more
CDN than
predicted from
CDN-aerosol
relation over
the Atlantic





AEROCOM microphysics working group

At 2008 AEROCOM workshop in Iceland, working group established to evaluate aerosol microphysics models against range of available in-situ observations.

Use syntheses of in-situ observations as benchmark to evaluate the models.

Evaluate & document diversity of AEROCOM models in simulated number conc'n

Common modelling experiments set up:

- Control simulation reference year 2006 (A2-CTRL-2006)
- As CTRL but with condensational growth switched off (A2-SIZ1-2006)
- As CTRL but with coagulation switched off (A2-SIZ2-2006)
- As CTRL but with primary emissions of SO₄ and BC/OC off (A2-SIZ3-2006)
- As CTRL but with new particle formation switched off (A2-SIZ4-2006)

A2-SIZ1, A2-SIZ2 compare role of growth processes in different models.

A2-SIZ3 allows multi-model assessment of contribution of primary particles to CCN

A2-SIZ4 allows multi-model assessment of nucleated CCN in different models.

Use HCA-0 emissions in models to minimise differences between model simulations.

Ask models to extend A2-CTRL-2006 through 2007 and 2008 to run through EUCAARI period with EUCAARI Different models



Challenges when evaluating number concentrations

Models characterise size distribution in many different ways

- mass-only in aerosol types each with fixed size distribution (~10 aerosol tracers)
- number & mass concentrations in size modes (20-30 aerosol tracers)
- number & mass in concentrations size bins (100-200 aerosol tracers)

CCN observations retrieve CCN at many different supersaturations

(and different models use different methods to calculate CCN concentrations).

CN measurements can use different minimum diameter (e.g. 3nm or 10nm).

Size distribution observations made across different size ranges.

Approach settled on at 2008 workshop:

Instead of asking for extra complicated diagnostics, just make life simple:

Ask modelers to write “all-aerosol-tracer” output to AEROCOM database

And to provide README file with information on how size is handled in model.

Then can compare CN, CCN, size-resolved N ensuring consistent methodology.

Also ask modellers to interpolate to selected sites outputting at hourly resolution

- makes separation into different air mass types possible
- generate statistics of size distribution over daily cycle
- how well do microphysics models reproduce new particle formation events?



Required output for aerosol microphysics group:

- Monthly-mean all-aerosol-tracer output on full 3D model grid (3D-M)
- Daily-mean all-aerosol-tracer output over vertical profile at sites (1D-D)
- Hourly-mean all-aerosol-tracer output at surface at sites (0D-H)

Use CMOR tables: Aerocom_table_1DD, Aerocom_table_0DH on website.

50 selected sites for high-temporal resolution all-aerosol-tracer data:

GAW & ARM sites (CPC, nephelometer, aethalometer, some with lidar)

Alert, Barrow, Bondville, Mauna Loa, Neumayer, Samoa, South Pole,
Southern Great Plains,

21 EUSAAR supersites (many with DMPS, AMS, lidar)

Aspreveten, Auchenworth, Birkenes, Cabauw, Finokalia, Harwell,
Hohenpeissenberg, Hyytiala, Ispra, Jungfrauoch, Kosetice, K-puzta,
Mace Head, Melpitz, Montseny, Moussala, Pallas, Preila, Puy de Dome,
Valvihill, Zeppelin.

Additional sites with observations

Cape Grim, Cape Point, Capo San Juan, Elandsfontein, Guangzhou, Manaus,
Monte Cimone, Mount Waliguan, Paverne, Shang Dianzi, Sonnblick, Summit,
Tahkuse, Trinidad Head, Varrio

Need model README file giving full detail of size assumptions with model



Global aerosol microphysics models in AEROCOM phase2

Many groups have now submitted the model all-aerosol-tracer data:

Model	Aerosol Dynamics	# of aerosol tracers	Contact
GLOMAP-mode	Modal (N,m)	26	Graham Mann (Leeds)
ECHAM-HAM2	Modal (N,m)	45 (20 SOA)	Kai Zhang (MPI-Hamburg)
GISS-TOMAS	Bin-resolved (N,m)	72	Yunha Lee (Carnegie Mellon)
GLOMAP-bin	Bin-resolved (N,m)	~200	Dominick Spracklen (Leeds)
EMAC [ECHAM-MESSy]	Modal (N,m)	30+	Kirsty Pringle (MPI-Mainz)
TM5	Modal (N,m)	25	Elisabetta Vignati (JRC)
PNNL-CAM5-MAM	Modal (N,m)	15	Xiaohong Liu (PNNL)
FMI-SALSA	Bin (N,m)	~70	Tommi Bergman (Univ Helsinki)
GISS-MATRIX	Moments (N,m)	60	Susanne Bauer (GISS)
CCCma AGCM4	PLA-bin (N,m)	240	Knut Van Salzen (Env Canada)
GEOS-CHEM-APM	Bin-resolved (N,m)	780	G. Luo & F. Yu (NY State Uni, Albany)
HadGEM3-UKCA	Modal (N,m)	26	Graham Mann (Leeds)

Also several mass-based models have submitted results, for which CN and CCN concentrations can be re-constructed and compared against those from the aerosol microphysics models.



Global aerosol microphysics models in AEROCOM phase2

Many groups have now submitted the model all-aerosol-tracer data:

Model	Aerosol Dynamics	# of aerosol tracers	Contact
GLOMAP-mode	Modal (N,m)	26	Graham Mann (Leeds)
ECHAM-HAM2	Modal (N,m)	45 (20 SOA)	Kai Zhang (MPI-Hamburg)
GISS-TOMAS	Bin-resolved (N,m)	72	Yunha Lee (Carnegie Mellon)
GLOMAP-bin	Bin-resolved (N,m)	~200	Dominick Spracklen (Leeds)
EMAC [ECHAM-MESSy]	Modal (N,m)	30+	Kirsty Pringle (MPI-Mainz)
TM5	Modal (N,m)	25	Elisabetta Vignati (JRC)
PNNL-CAM5-MAM	Modal (N,m)	15	Xiaohong Liu (PNNL)
FMI-SALSA	Bin (N,m)	~70	Tommi Bergman (Univ Helsinki)
GISS-MATRIX	Moments (N,m)	60	Susanne Bauer (GISS)
CCCma AGCM4	PLA-bin (N,m)	240	Knut Van Salzen (Env Canada)
GEOS-CHEM-APM	Bin-resolved (N,m)	780	G. Luo & F. Yu (NY State Uni, Albany)
HadGEM3-UKCA	Modal (N,m)	26	Graham Mann (Leeds)

Also several mass-based models have submitted results, for which CN and CCN concentrations can be re-constructed and compared against those from the aerosol microphysics models.



Assembled benchmark observational datasets.

Wide range of observational datasets being used at Leeds to evaluate the bin and modal versions of GLOMAP.

- 1) CN concentrations from CPC observations at GAW & other sites
- 2) size-resolved number concentrations & mean size against compilations of multiple field campaign measurements (e.g. Heintzenberg et al, 2000, 2004).
- 3) vertical CN, CCN profiles from models against compilations of aircraft observations (e.g. TRACE-P, PEM-Tropics, INCA, UFA-EXPORT, LACE field campaigns)
- 4) CCN concentrations from field campaigns and monitoring sites.
- 5) size distributions against DMPS observations at EUSAAR sites

Evaluate AEROCOM size-resolving global aerosol models.

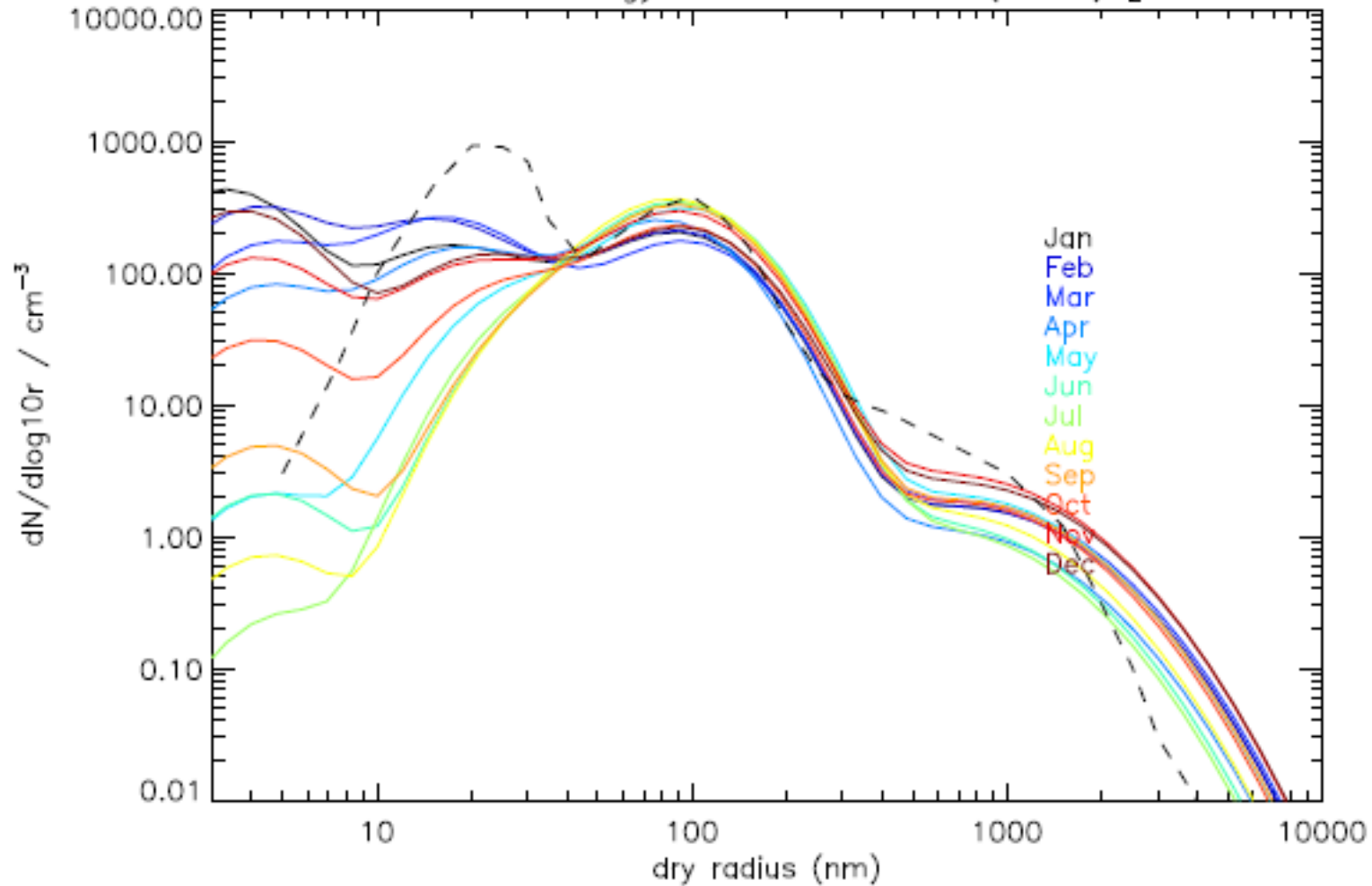
Use mean-bias and correlation coefficient to score models

Provide observational constraint for simulated size distribution.



GLOMAP-mode v4 vs marine BL size distribution (Raes00)

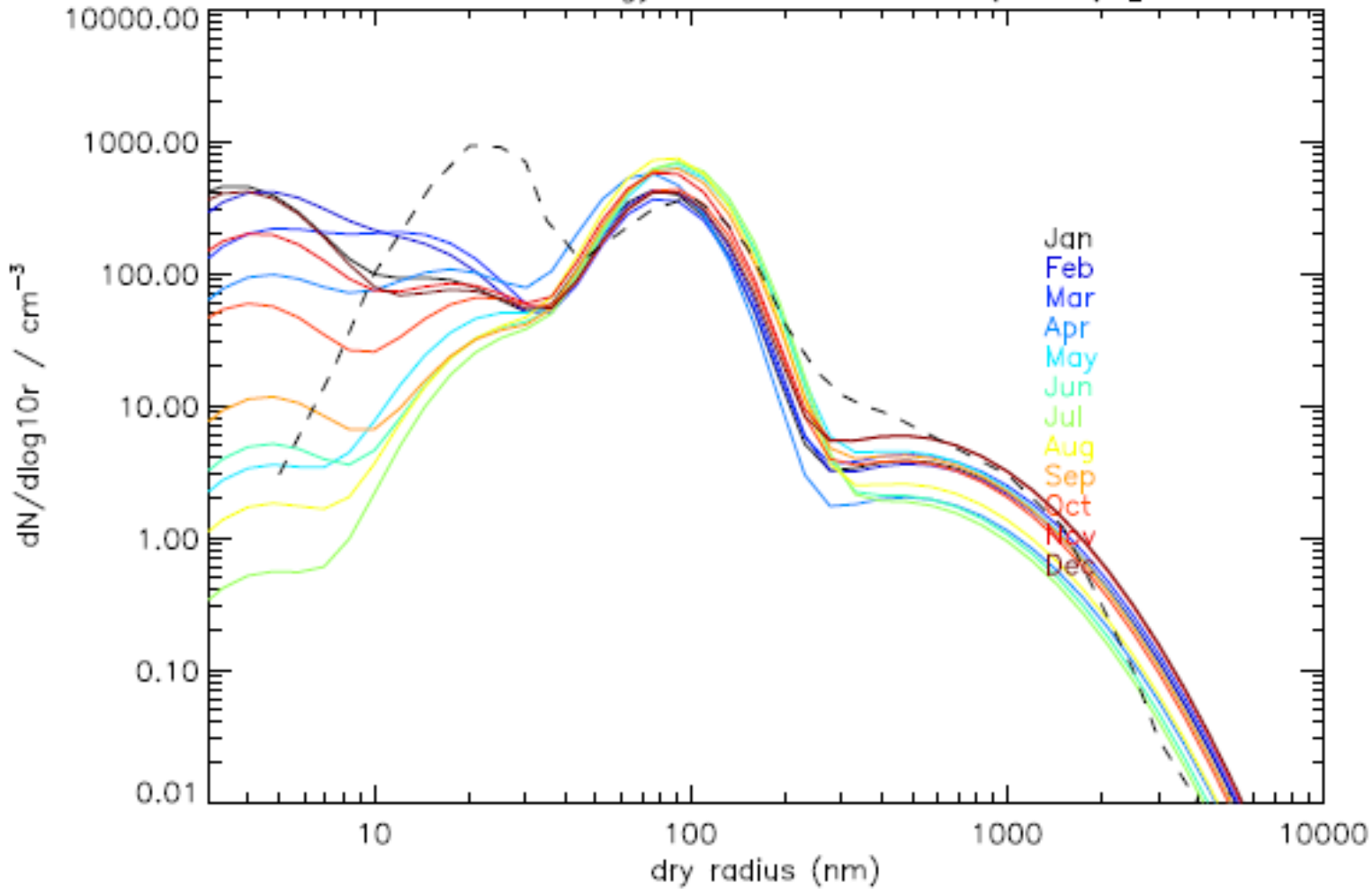
GLOMAP-mode c.f. obs climatology from Raes et al (2000) [N. Atlantic MBL July]





GLOMAP-mode v6R vs marine BL size distribution (Raes00)

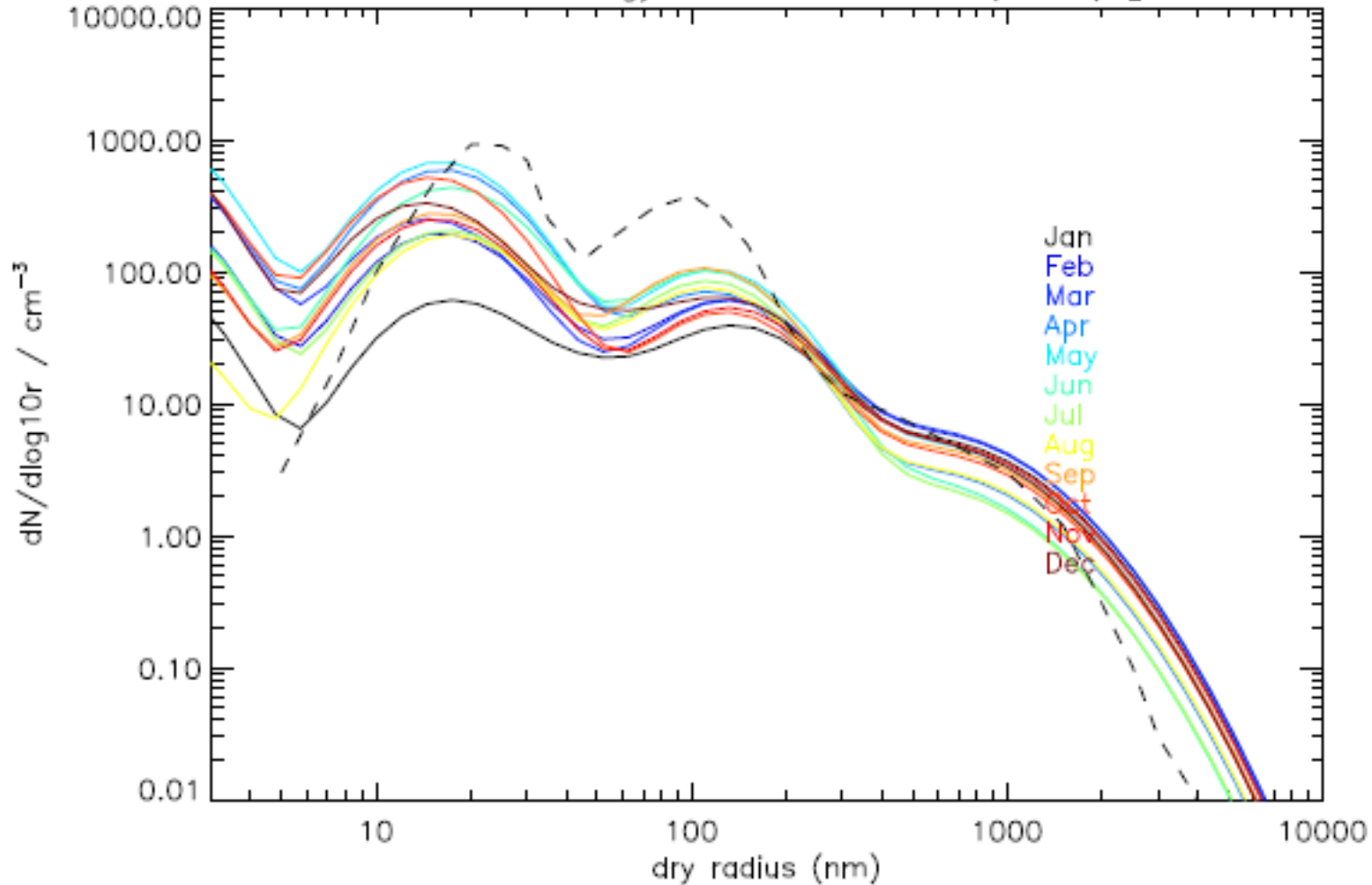
GLOMAP-mode c.f. obs climatology from Raes et al (2000) [N. Atlantic MBL July]





ECHAM-HAM2 vs marine BL size distribution (Raes00)

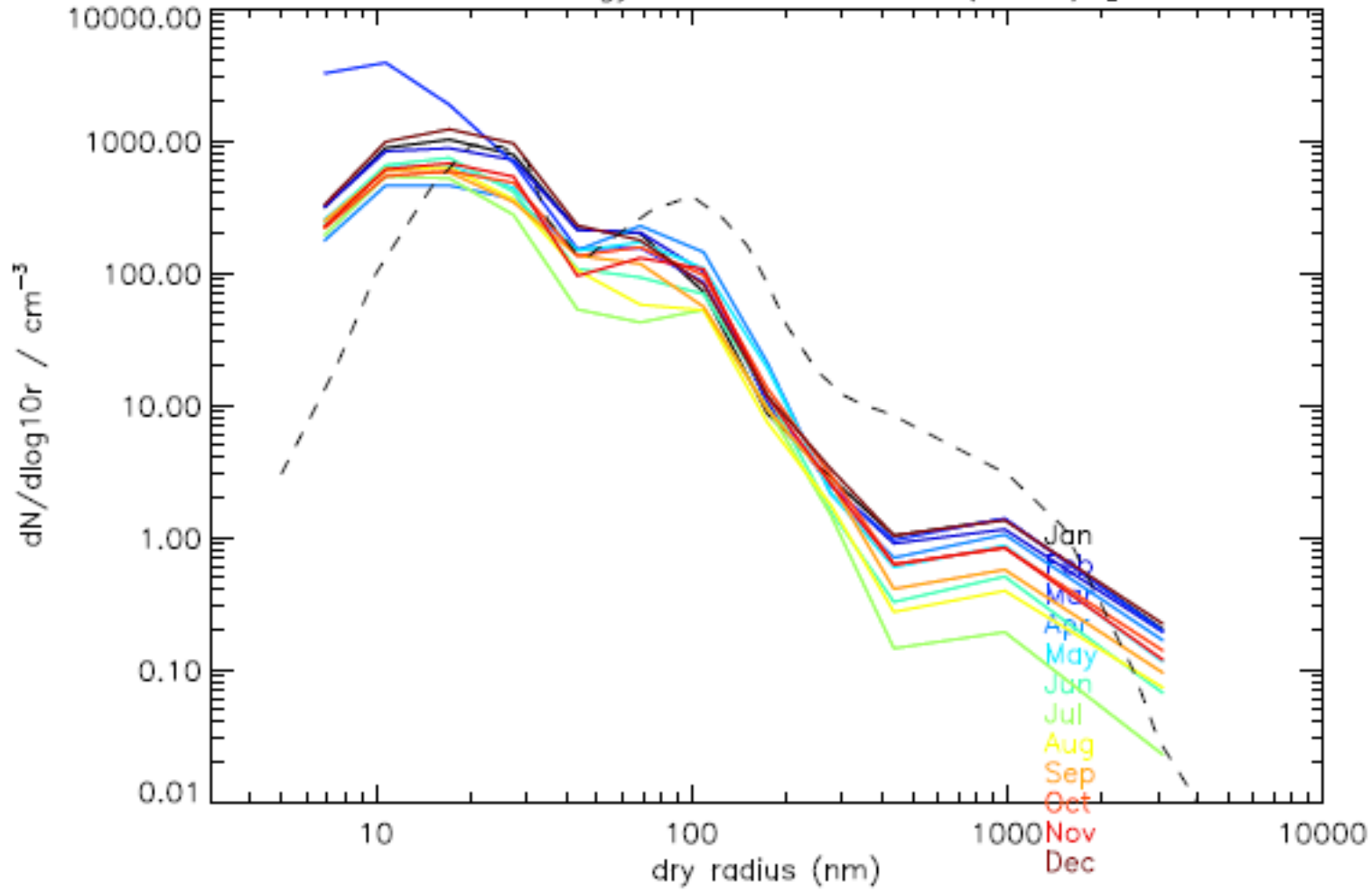
GLOMAP-mode c.f. obs climatology from Raes et al (2000) [N. Atlantic MBL July]





GISS-TOMAS vs marine BL size distribution (Raes00)

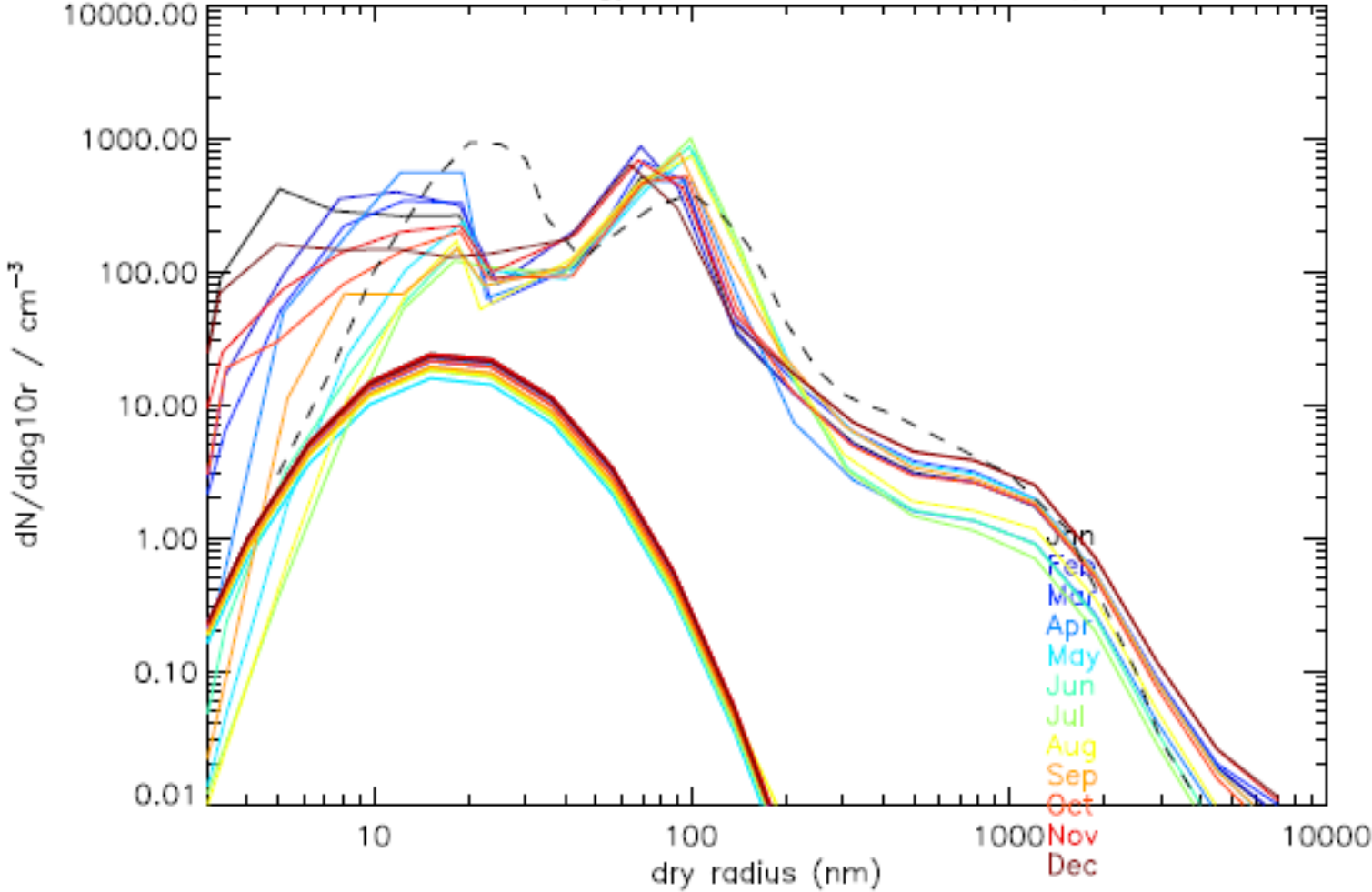
GLOMAP-bin c.f. obs climatology from Raes et al (2000) [N. Atlantic MBL July]





GLOMAP-bin vs marine BL size distribution (Raes00)

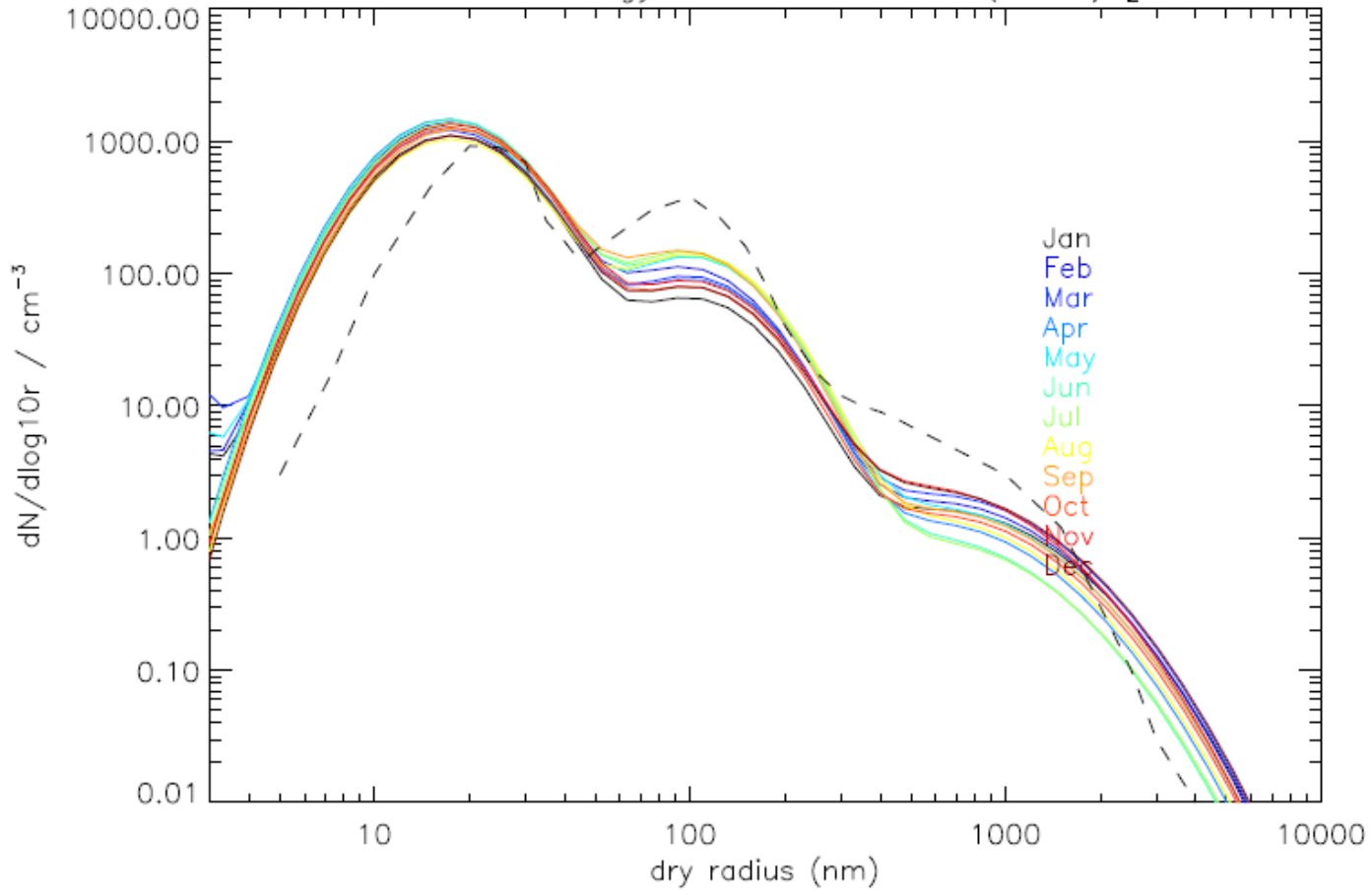
GLOMAP-bin c.f. obs climatology from Raes et al (2000) [N. Atlantic MBL July]





TM5-HAM vs marine BL size distribution (Raes00)

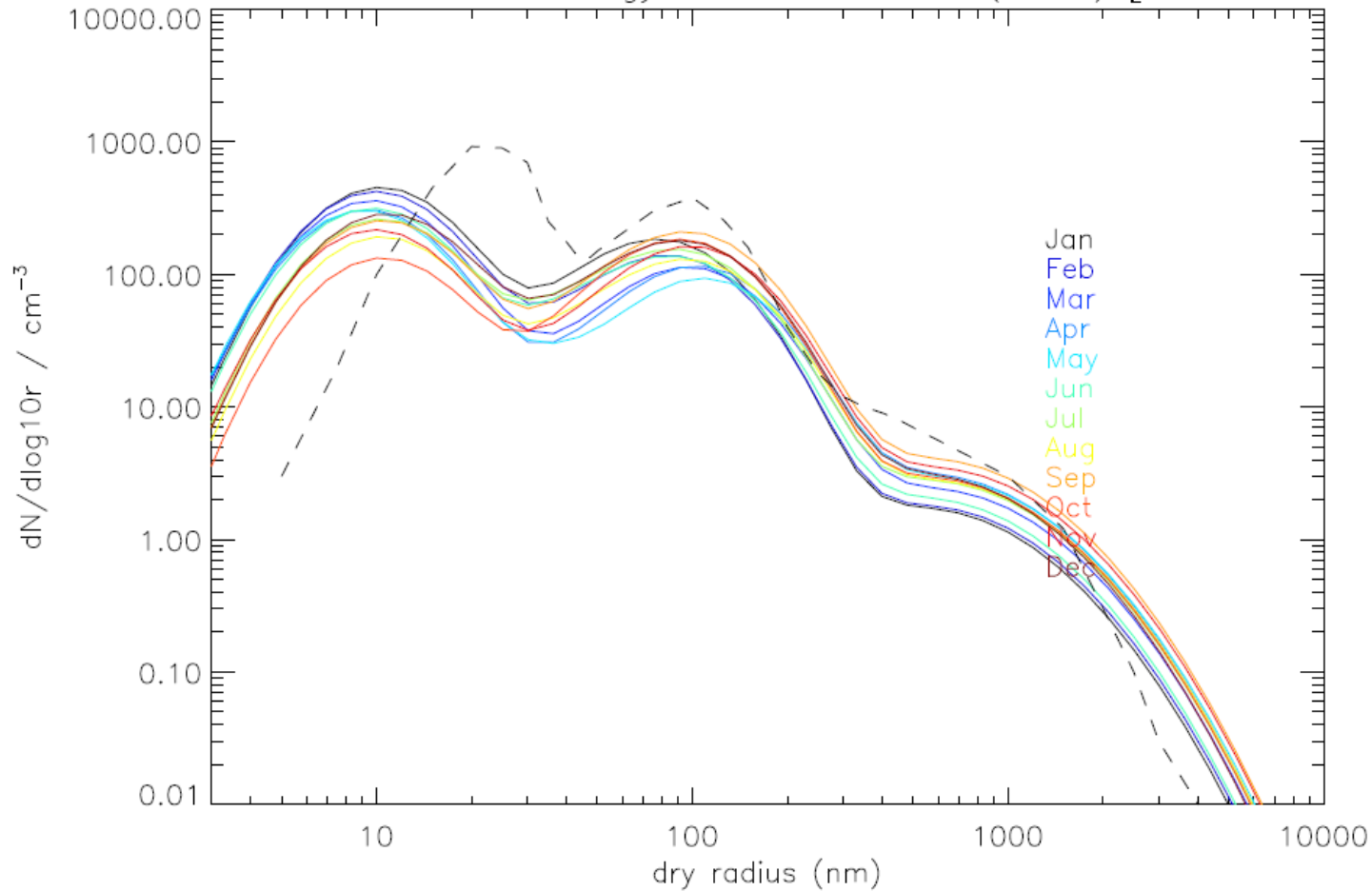
GLOMAP—mode c.f. obs climatology from Raes et al (2000) [N. Atlantic MBL July]





ECHAM-MESSY-GMXe vs marine BL size distribution (Raes00)

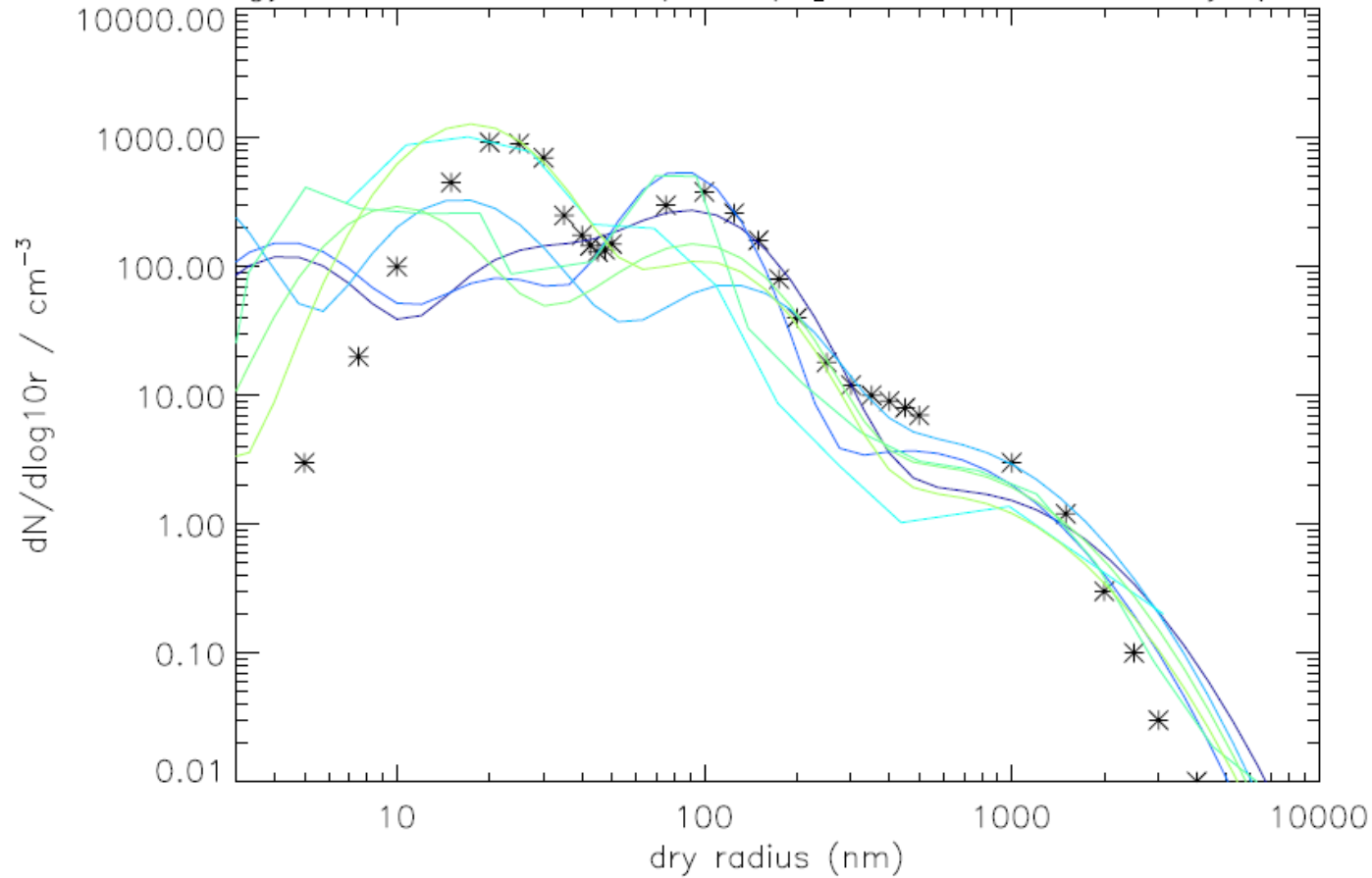
GLOMAP-mode c.f. obs climatology from Raes et al (2000) [N. Atlantic MBL Ju





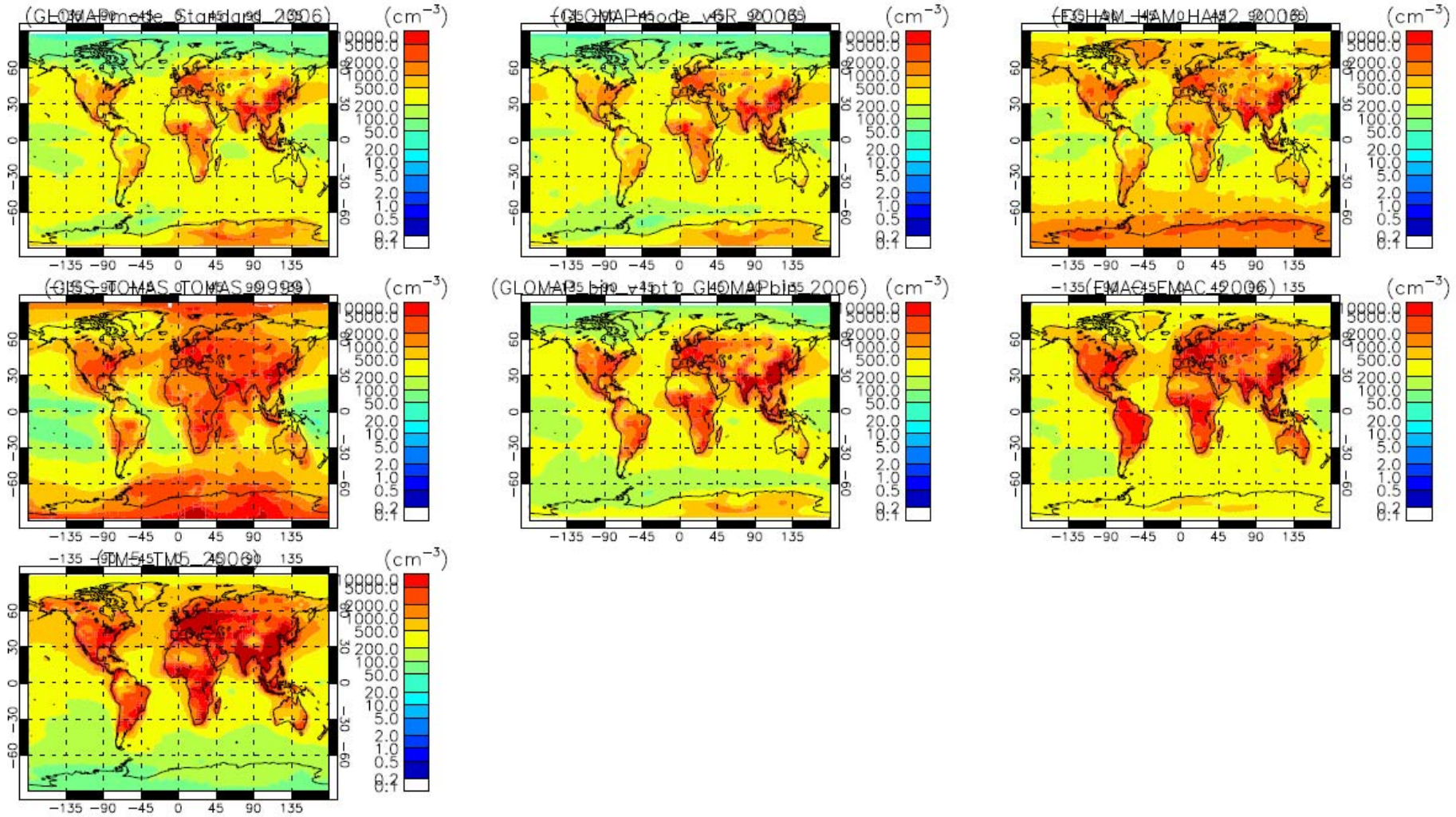
Diversity in simulated MBL size distributions

obs climatology from Raes et al (2000) [N. Atlantic MBL July (30–35W,



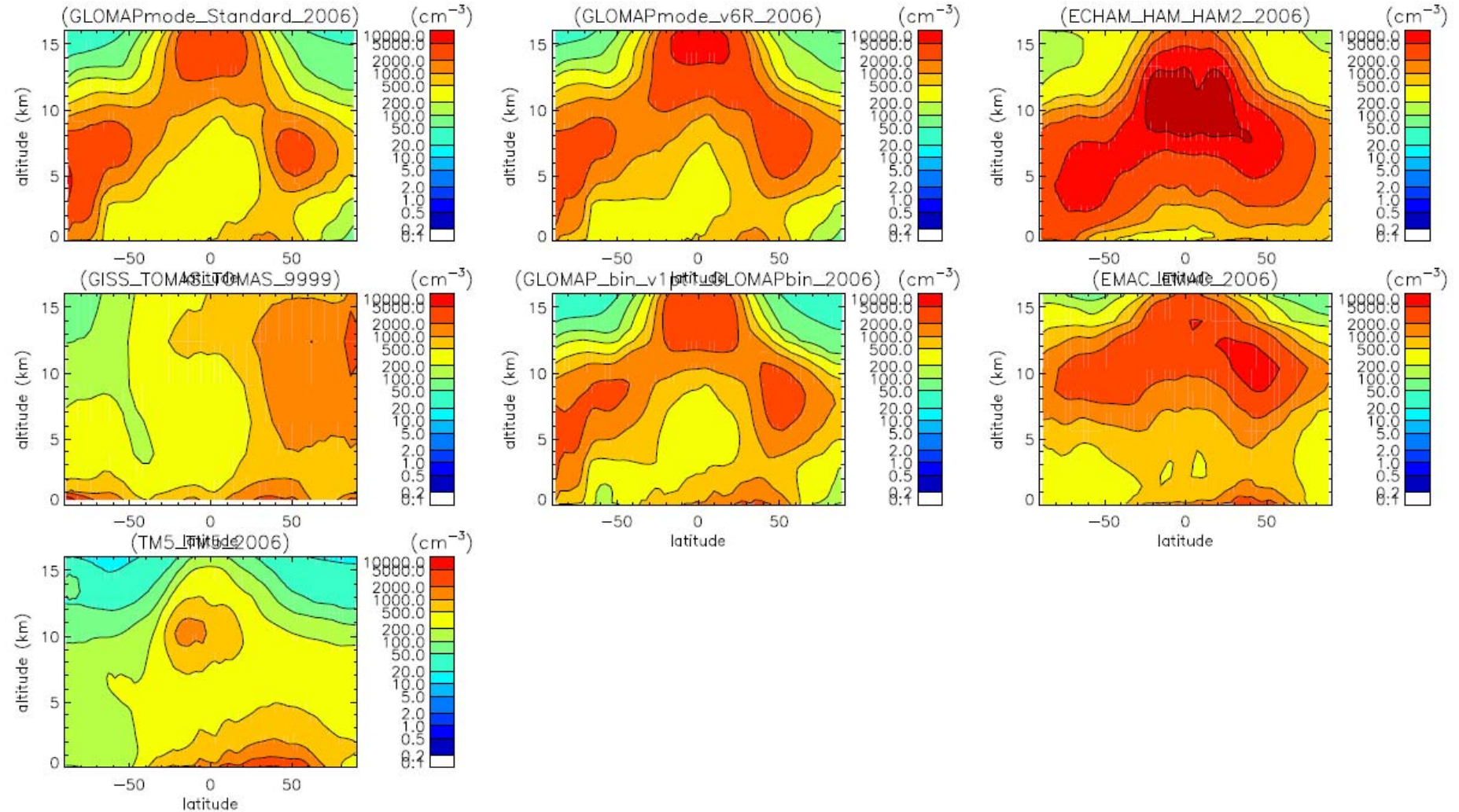


Diversity in simulated CN concentrations



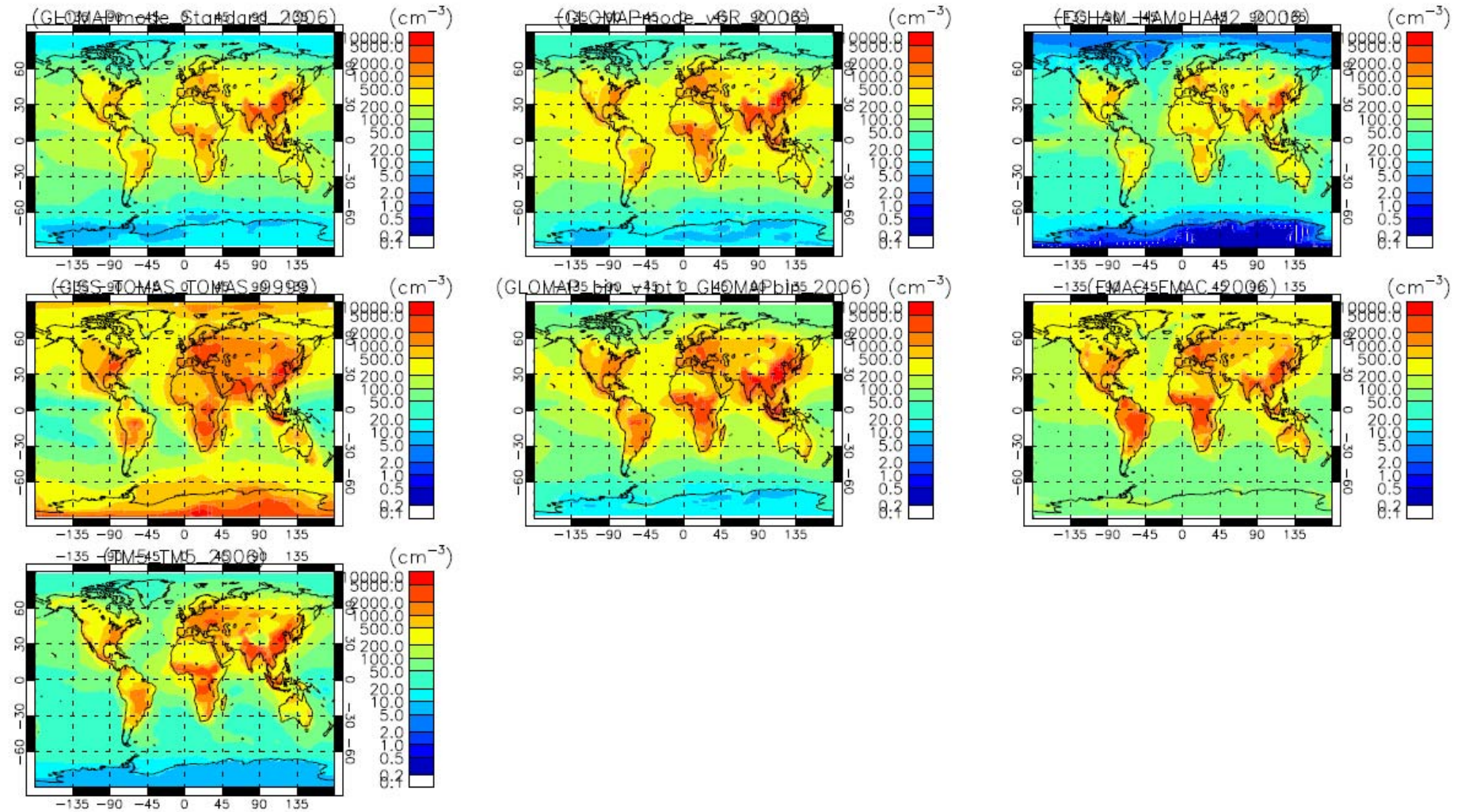


Diversity in simulated CN concentrations



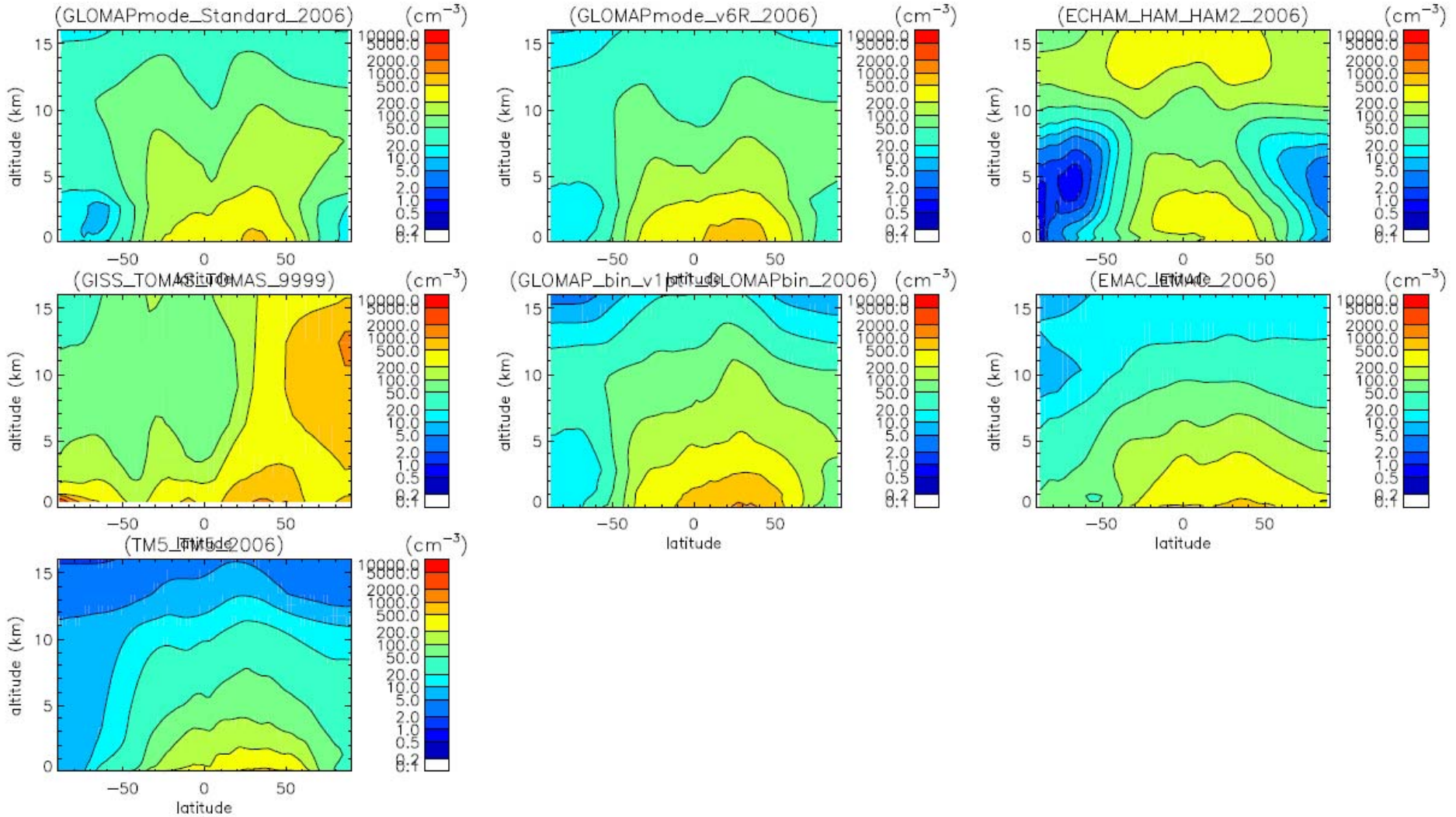


Diversity in simulated CCN concentrations



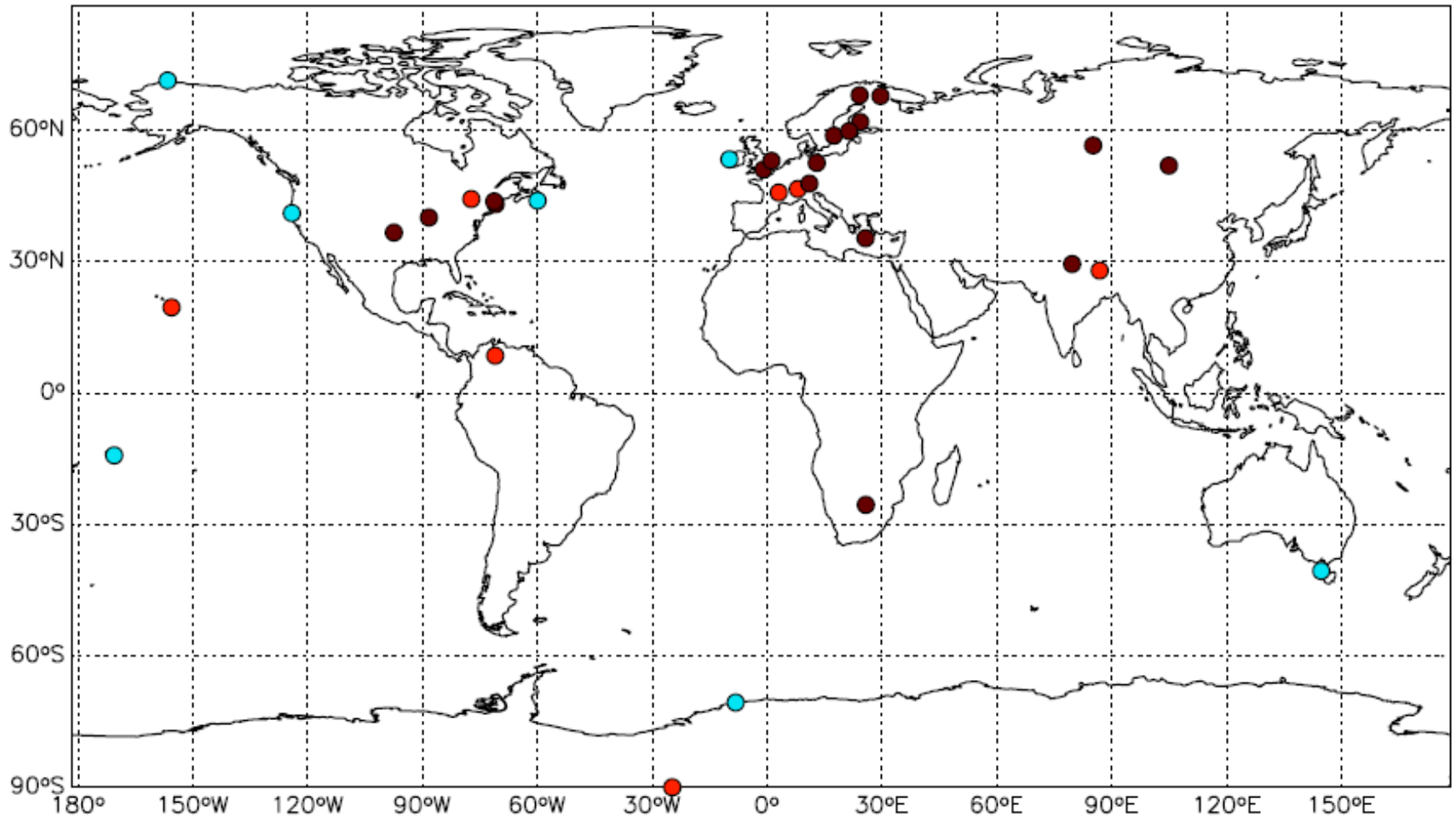


Diversity in simulated CCN concentrations





1. CN concentrations from GAW and other sites

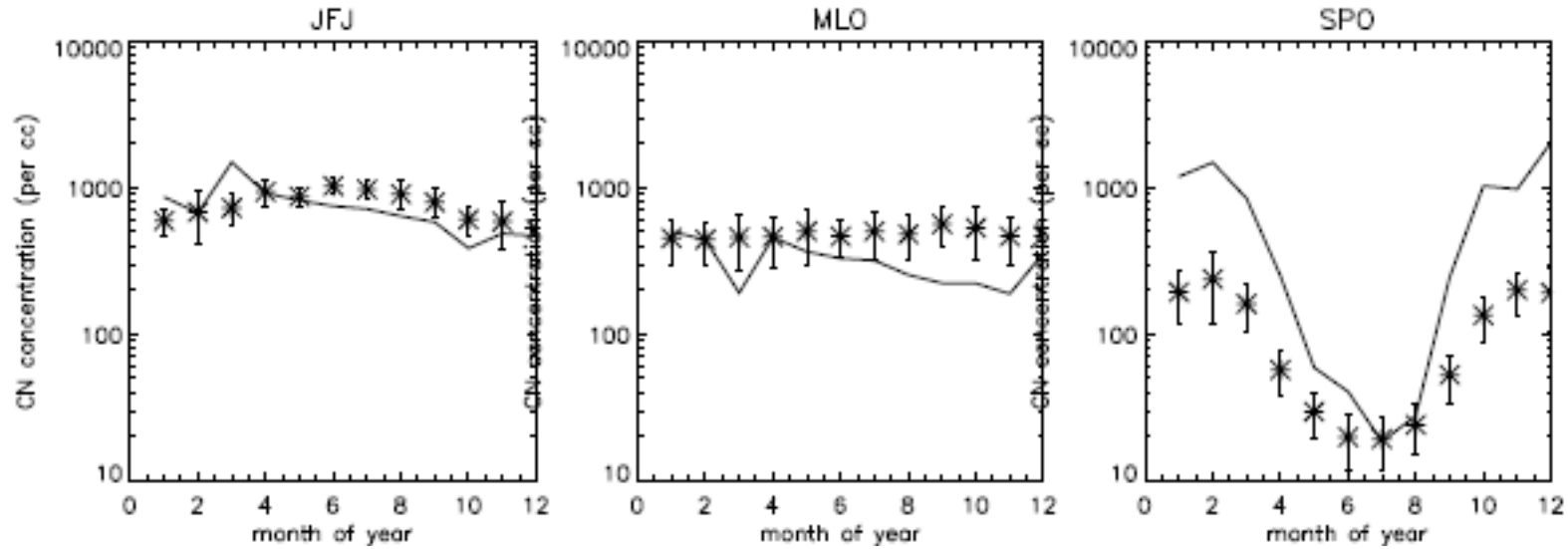


Remote marine BL sites

Continental BL sites

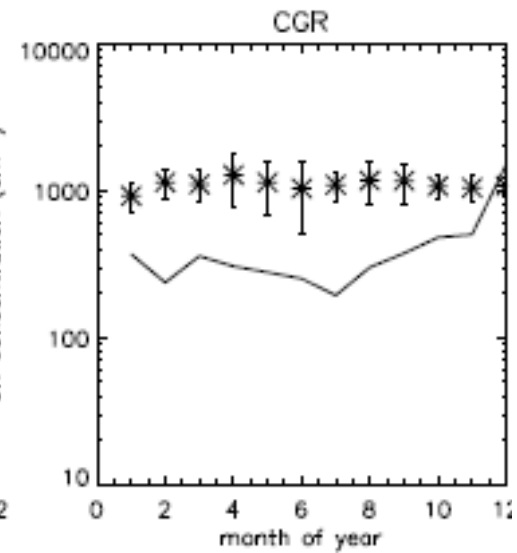
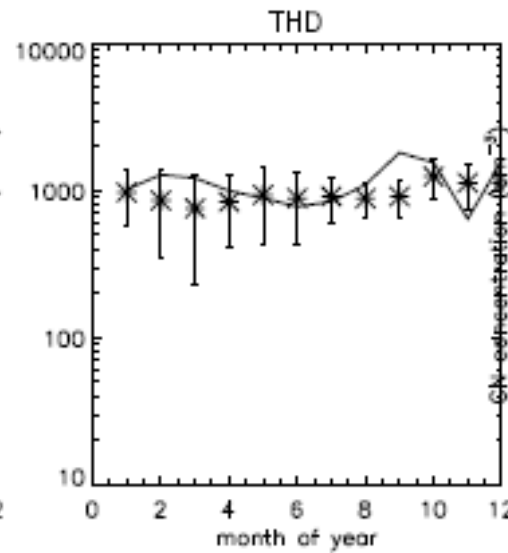
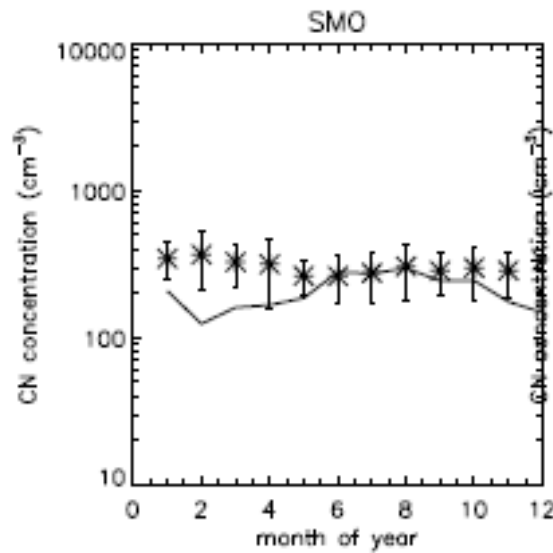
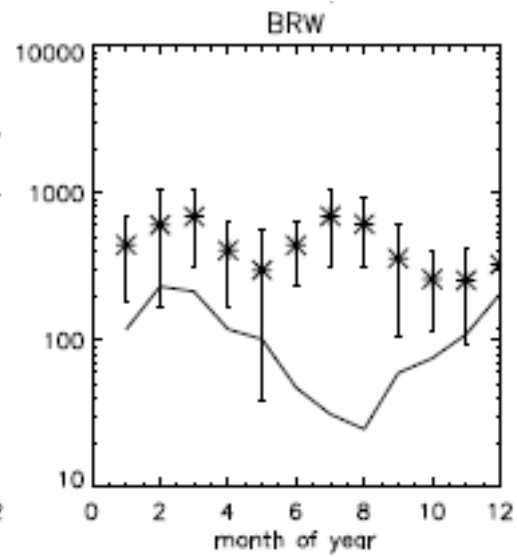
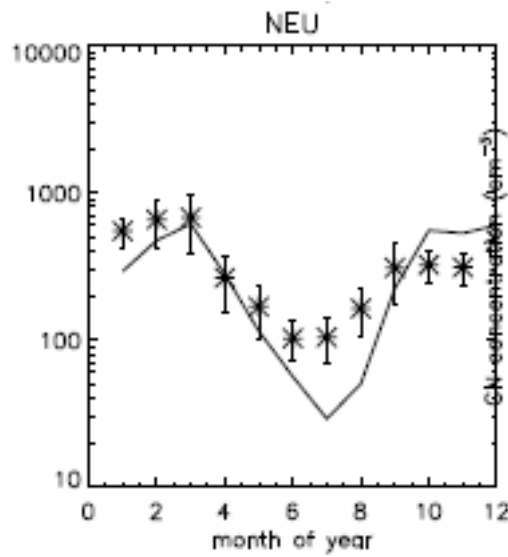
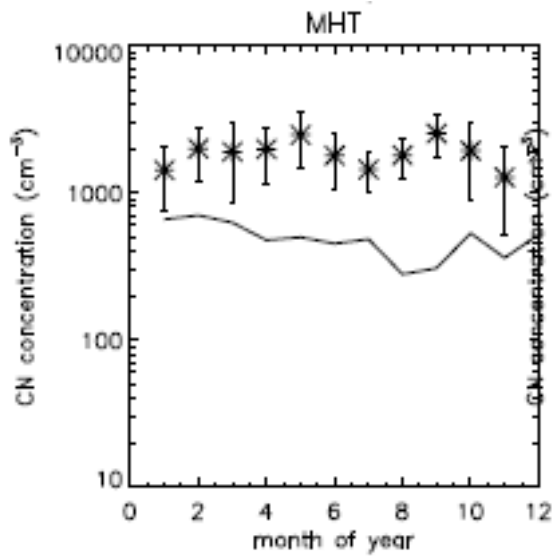
Free Troposphere sites

GLOMAP-bin vs CN annual cycle GAW sites (FT)





GLOMAP-mode v4 vs CN annual cycle GAW sites (MBL)



2. Compilation of MBL aerosol observations

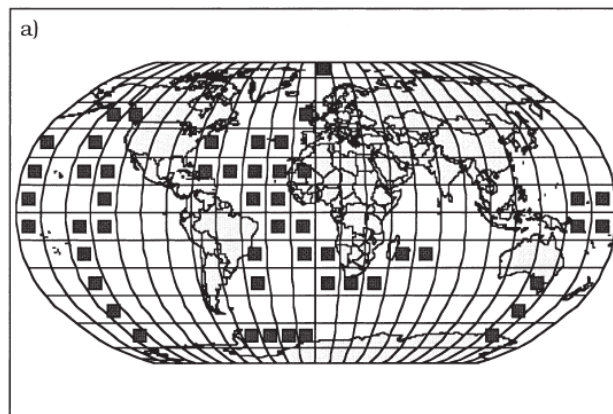
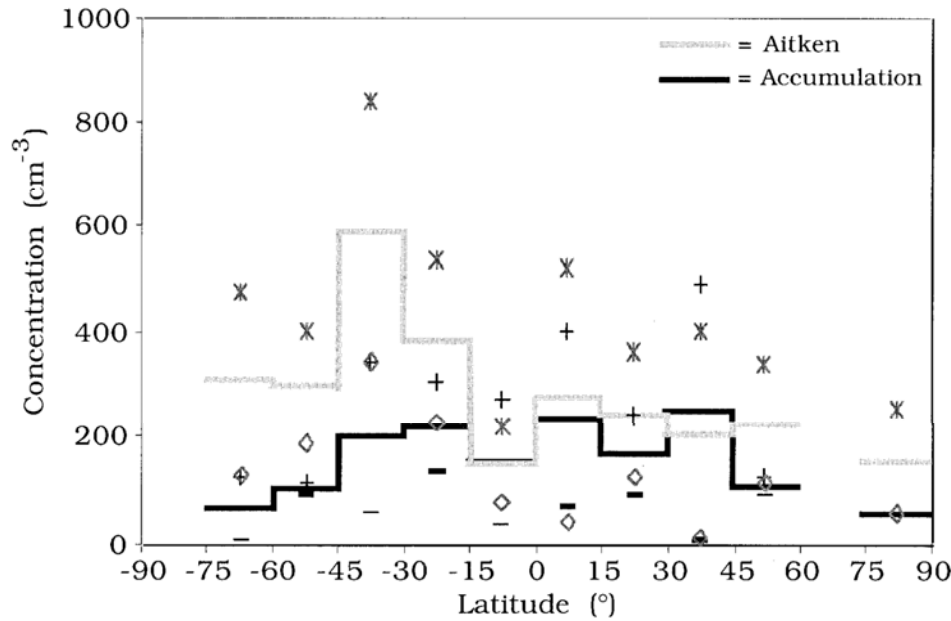


Table 1. Sources of data on aerosol concentration and number-size distribution

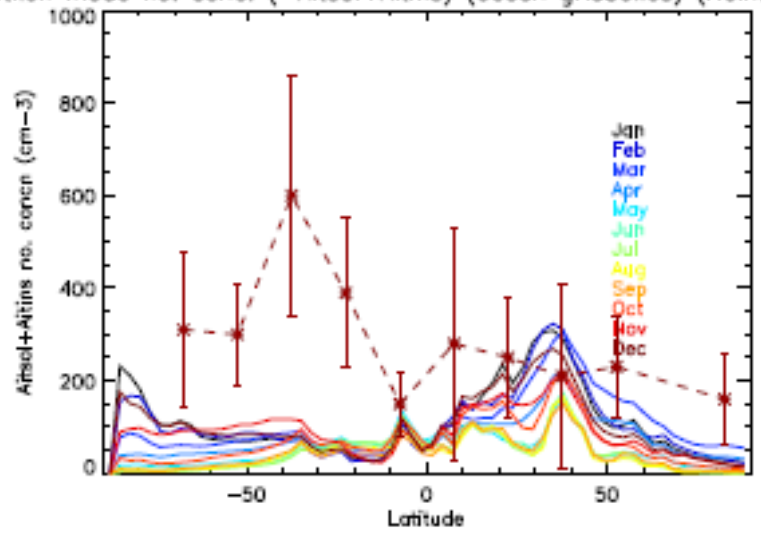
Source	Geographical area/ experiment
Bates et al, 1998b	Tasman Sea, Southern Ocean, ACE 1
Covert et al, 1996b	Arctic, IAOE91
Covert et al, 1996a	Central Pacific, MAGE
Covert et al. (unpublished data)	Equatorial Western Pacific, CSP
Davison et al, 1996a	Southern Ocean
Heintzenberg and Leck, 1994	Arctic
Jaenicke et al, 1992	Southern Ocean
Jensen et al, 1996	North E Atlantic, ASTEX
Leitch et al, 1996	NW Atlantic
Quinn et al, 1990	Central N Pacific, MAGE
Quinn et al, 1993	Central Eastern Pacific, MAGE
Quinn et al, 1995	Central Pacific, MAGE
Quinn et al, 1996	Central Pacific, MAGE
Raes et al, 1997	Tenerife
Van Dingenen et al, 1995	North Atlantic
Van Dingenen et al. (unpublished data)	Tenerife, ACE 2
Wiedensohler et al. (unpublished data)	Tasman Sea, Southern Ocean, ACE 1
Nowak et al. (unpublished data)	North and South Atlantic, Indic, AEROCRUISE 1999

Heintzenberg et al
(2000, Tellus B)

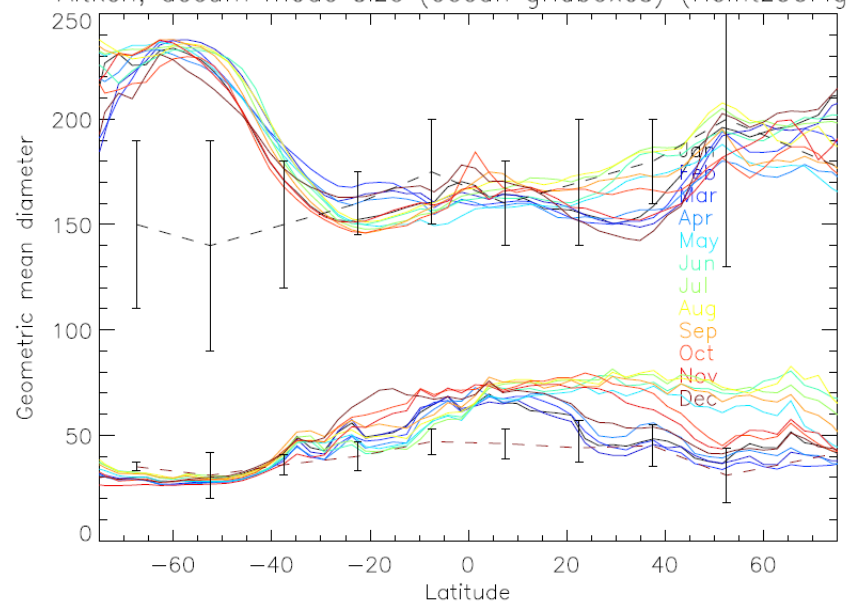


GLOMAP-mode v4 vs marine N_{Ait} & N_{acc} vs latitude (Heintz00)

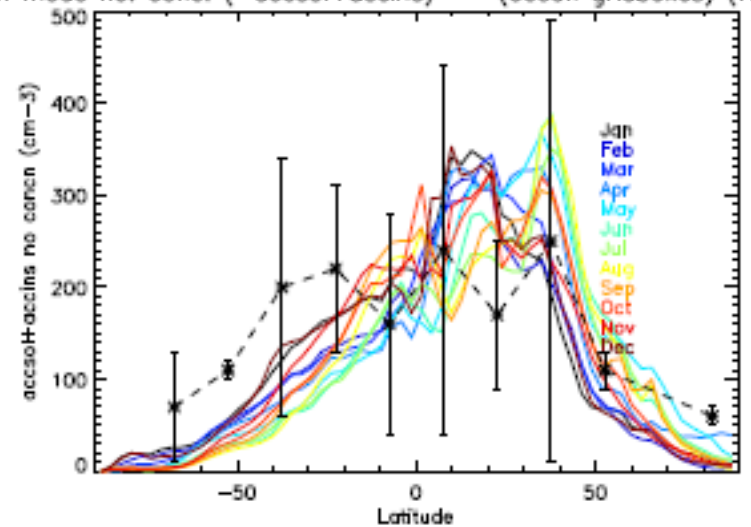
Aitken mode no. conc. (=A_{itsol}+A_{itins}) (ocean gridboxes) (Heintz00Fig3)



Aitken, accum mode size (ocean gridboxes) (Heintz00Fig4)



accum mode no. conc. (=a_{ccsol}+a_{ccins}) -- (ocean gridboxes) (Heintz00Fig)





3. Vertical profiles of size-resolved number conc

Aircraft observations

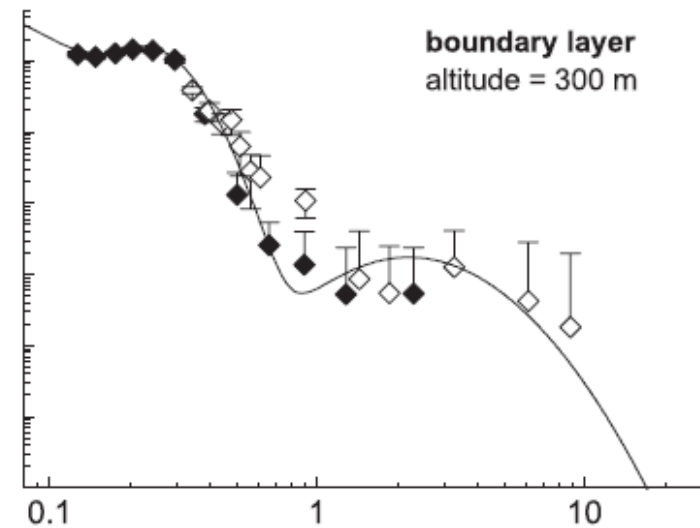
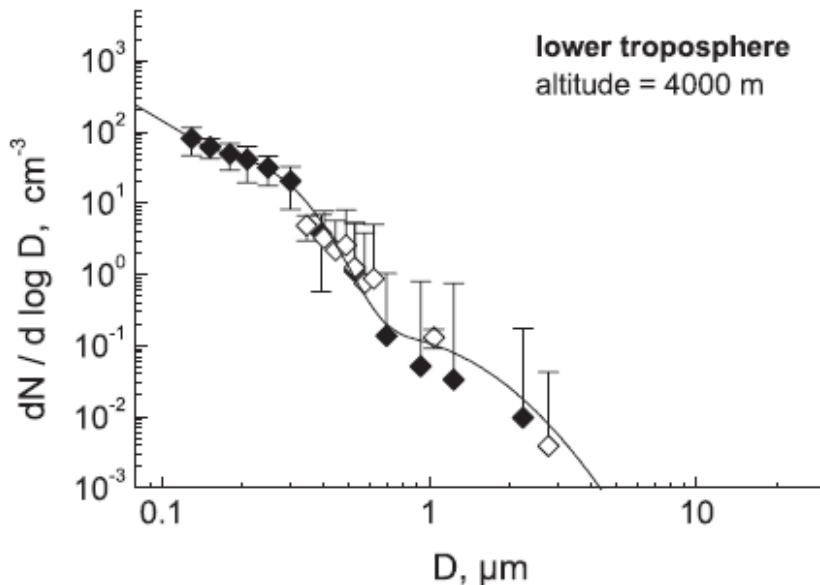
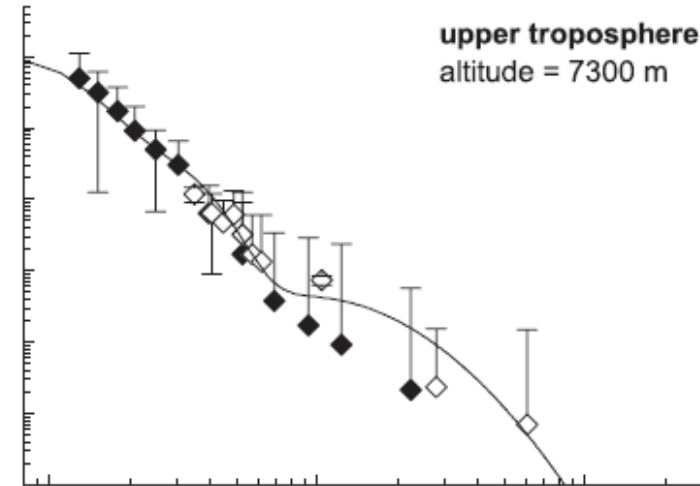
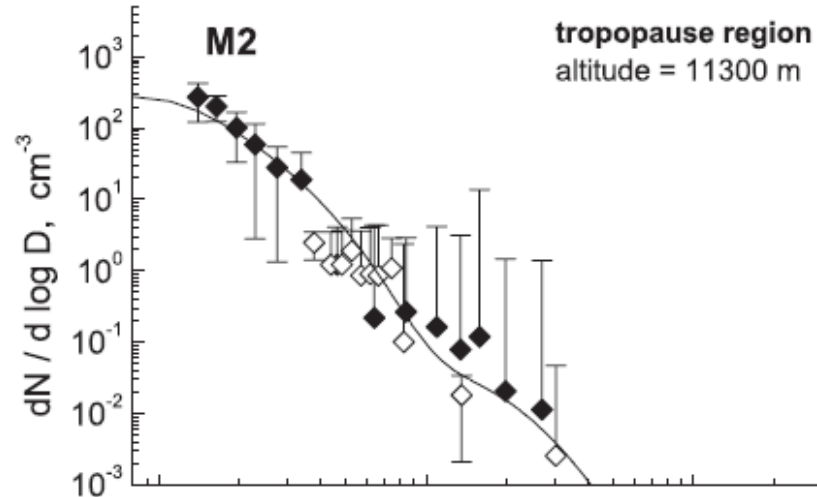
Continental Europe (Germany)

LACE campaign – Petzold et al (2002)

Marine regions (Pacific and Southern Oceans)

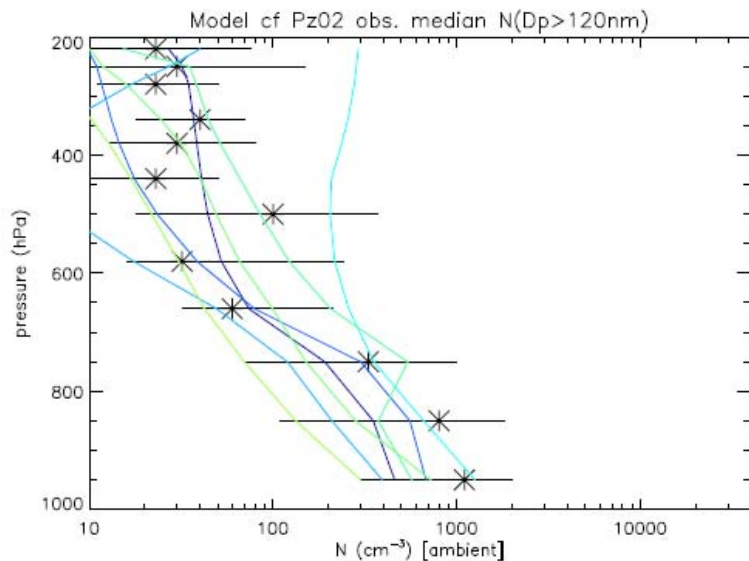
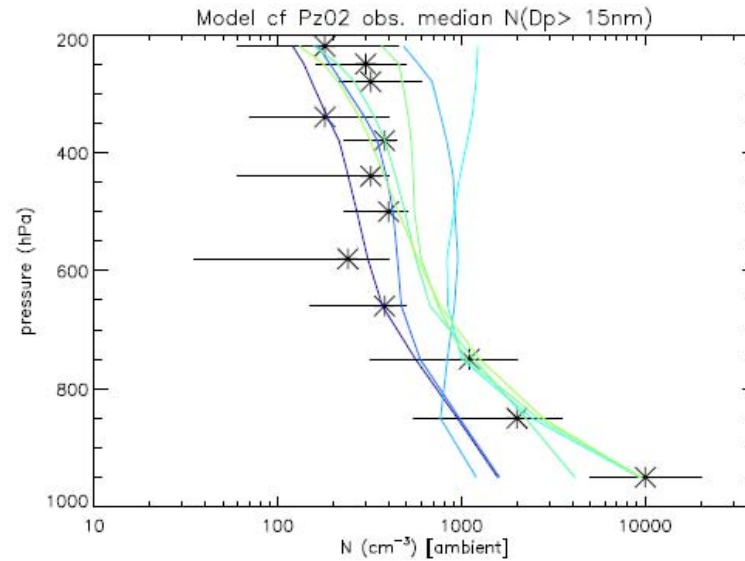
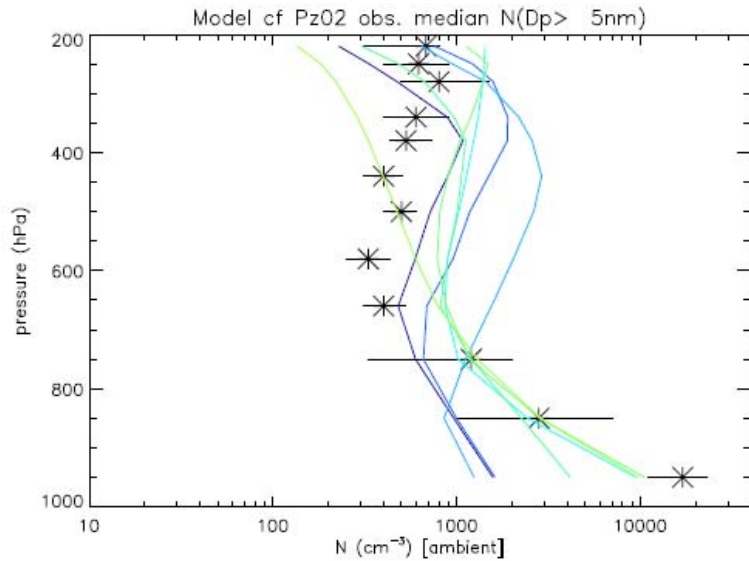
Several field campaigns – Clarke & Kapustin (2002)

Lindenberg Aerosol Characterization Experiment (LACE) Size distribution from PCASP and FSSP on DLR-Falcon



LACE profiles compiled by Lauer et al (2005) into datasets against which to test models

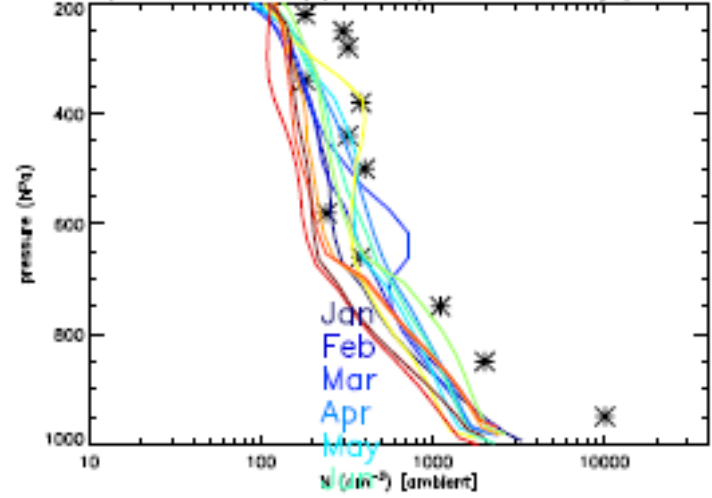
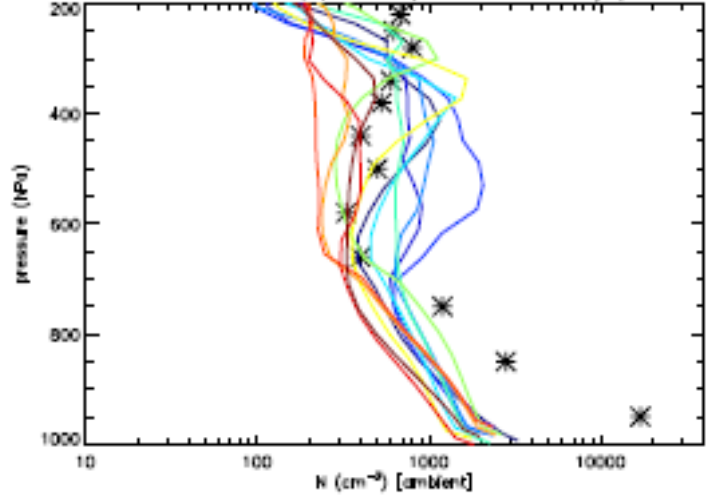
Lindenberg Aerosol Characterization Experiment (LACE) Size distribution from PCASP and FSSP on DLR-Falcon



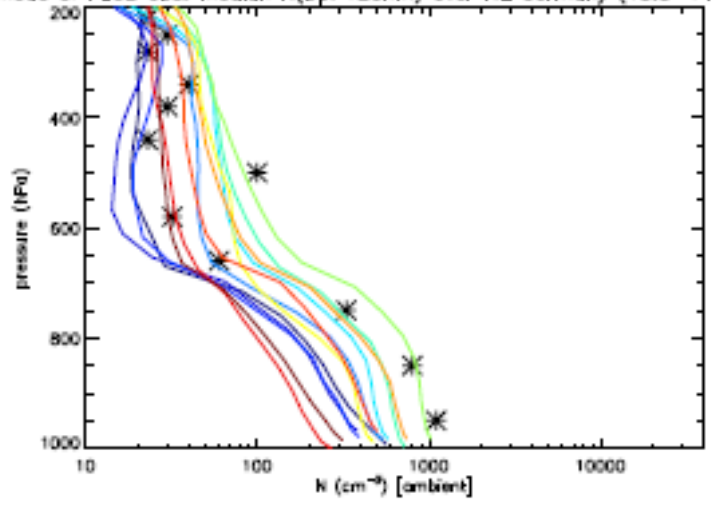


GLOMAP-mode v4 vs N(Dp>5,15,120nm) LACE campaign

GLOMAP-mode of Pz02 obs. median N(Dp> 5nm) over NE Germany (13.5-14.5E, 51.5-52.7N) vs Pz02 obs. median N(Dp> 15nm) over NE Germany (13.5-14.5E, 51.5-52.7N)

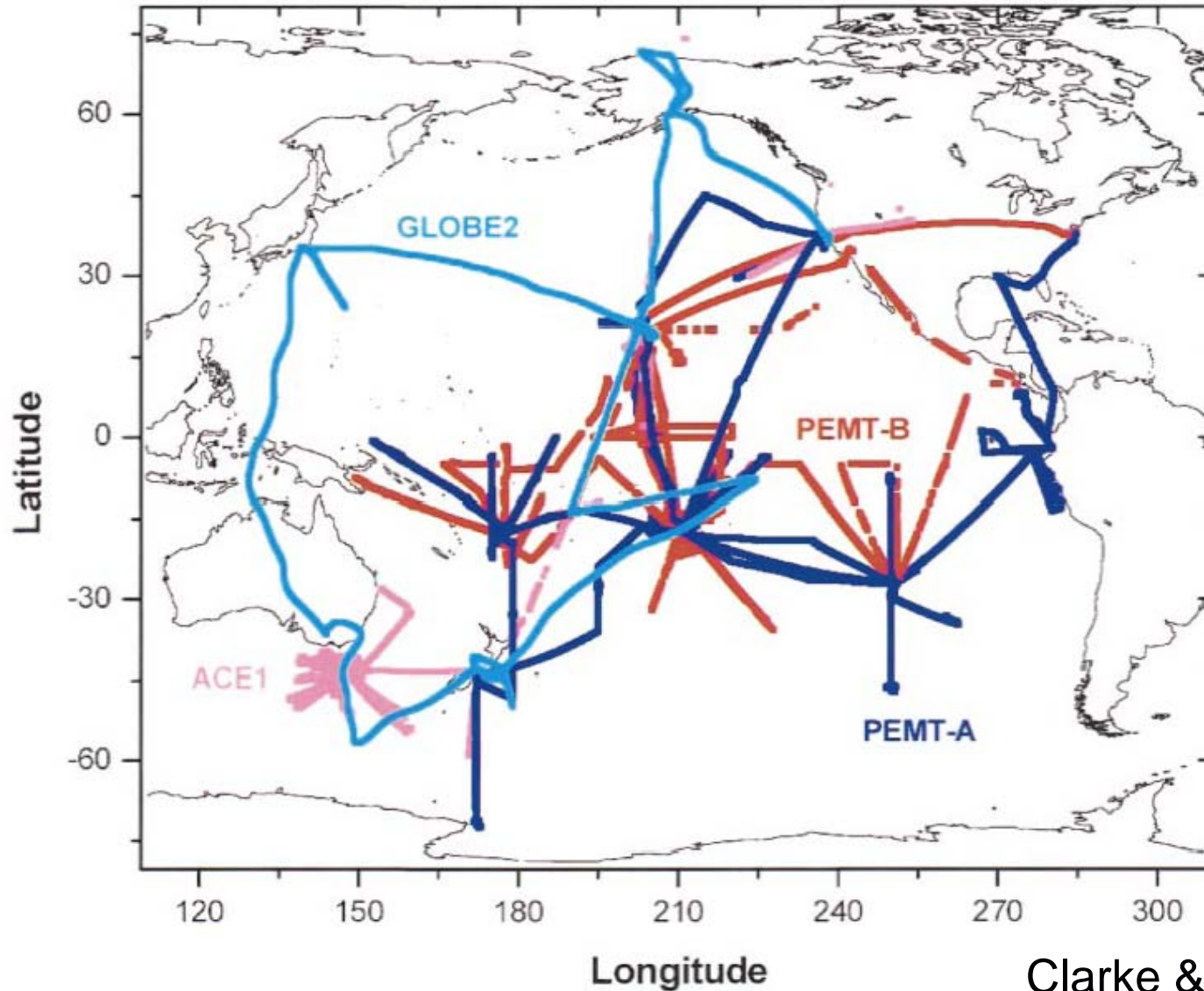


GLOMAP-mode of Pz02 obs. median N(Dp>120nm) over NE Germany (13.5-14.5E, 51.5-52.7N)



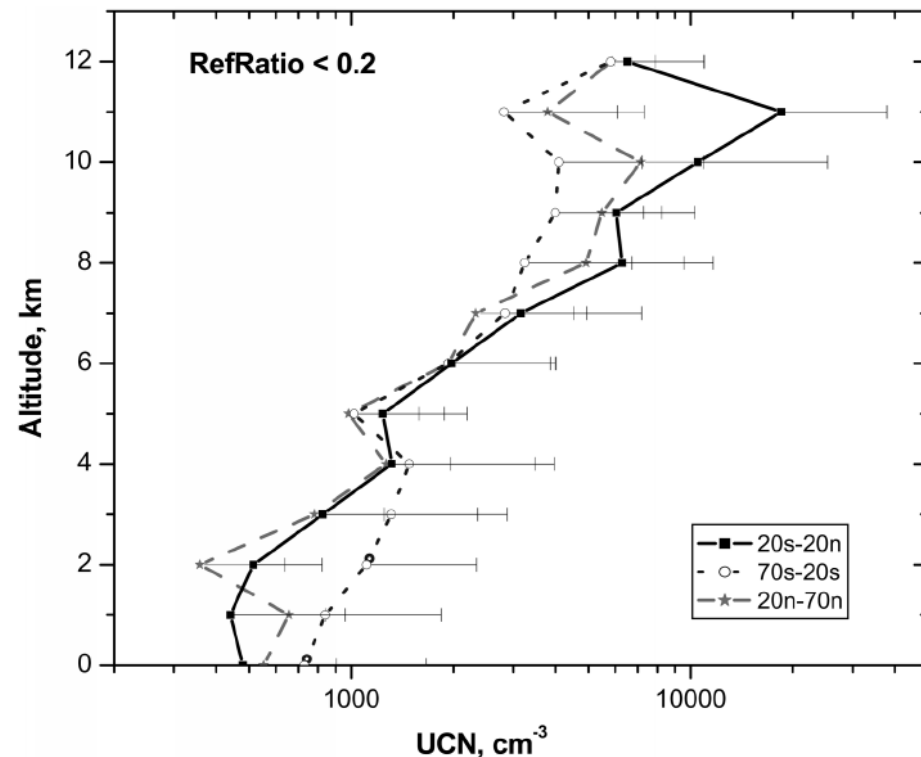
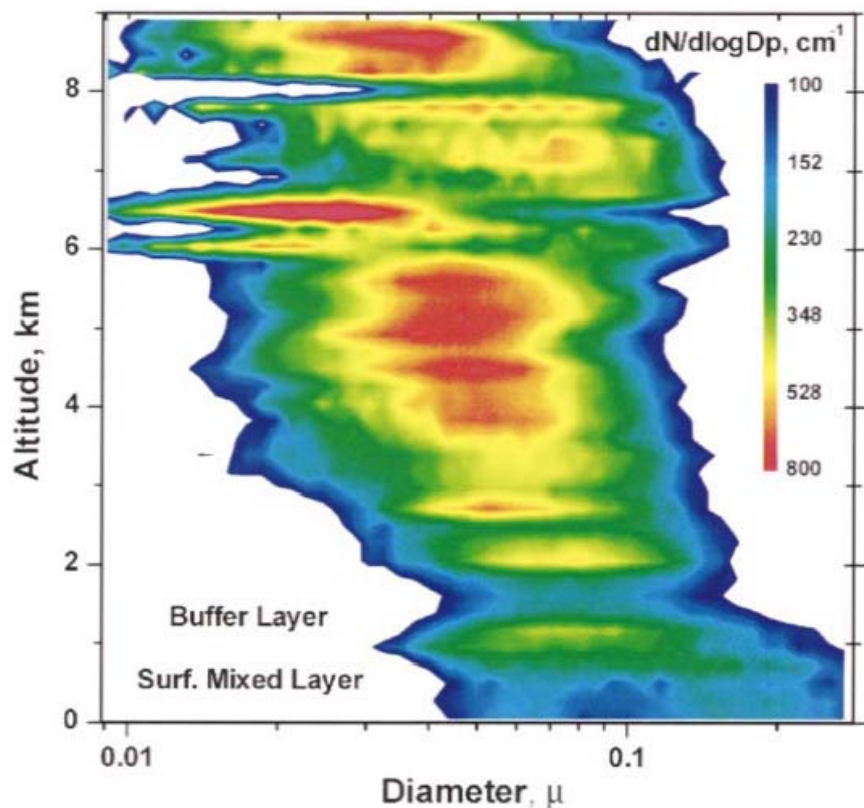
Jan
Feb
Mar
Apr
May
Jun
Jul
Aug
Sep
Oct
Nov
Dec

Compilation of aircraft-borne CNC measurements from several field campaigns



Clarke & Kapustin (2002)

Compilation of aircraft-borne CNC measurements from several field campaigns



Size distributions unimodal in FT growing from 5km \rightarrow 2km over Pacific.
Bi-modal MBL size distributions with Hoppel gap following cloud processing.

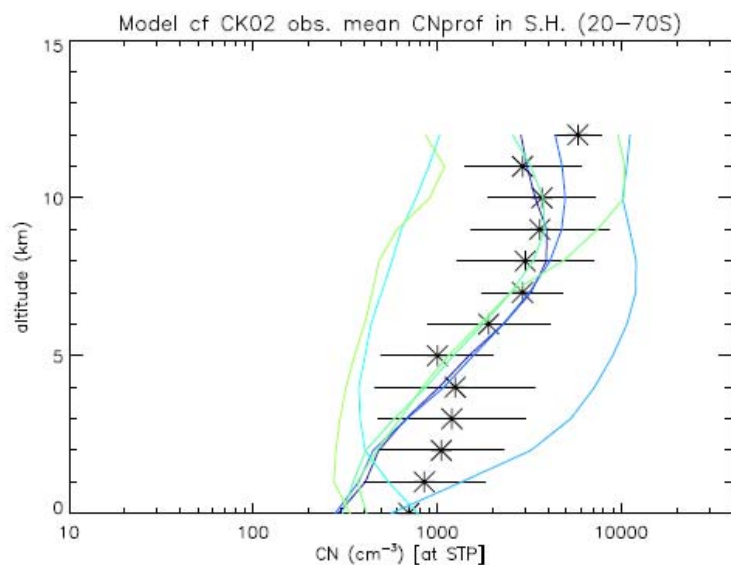
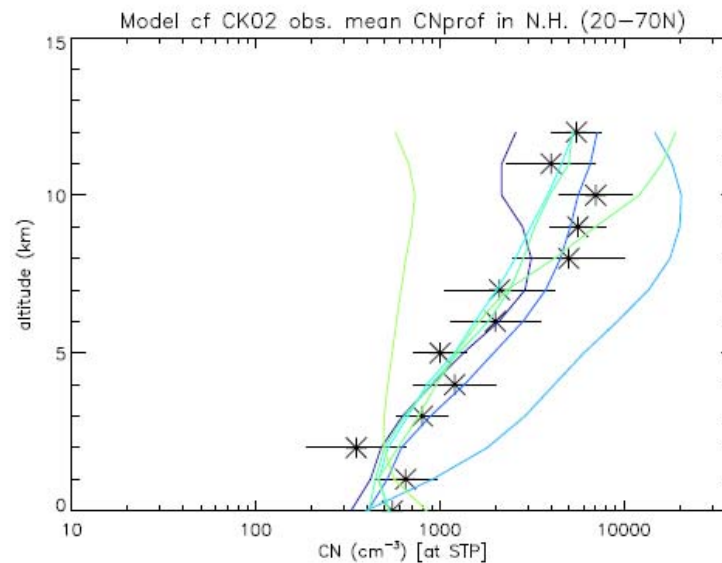
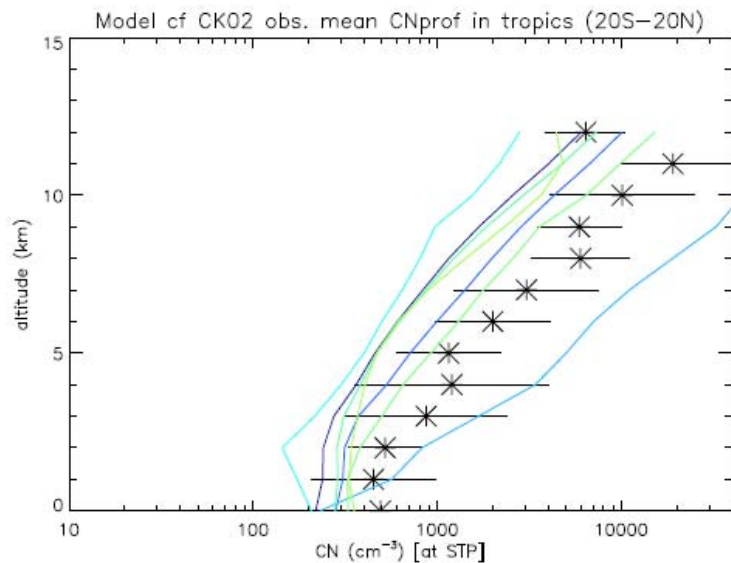
CN peak in FT – nucleation layer.

Clarke & Kapustin (2002)

Compilation of aircraft-borne CNC measurements from several field campaigns



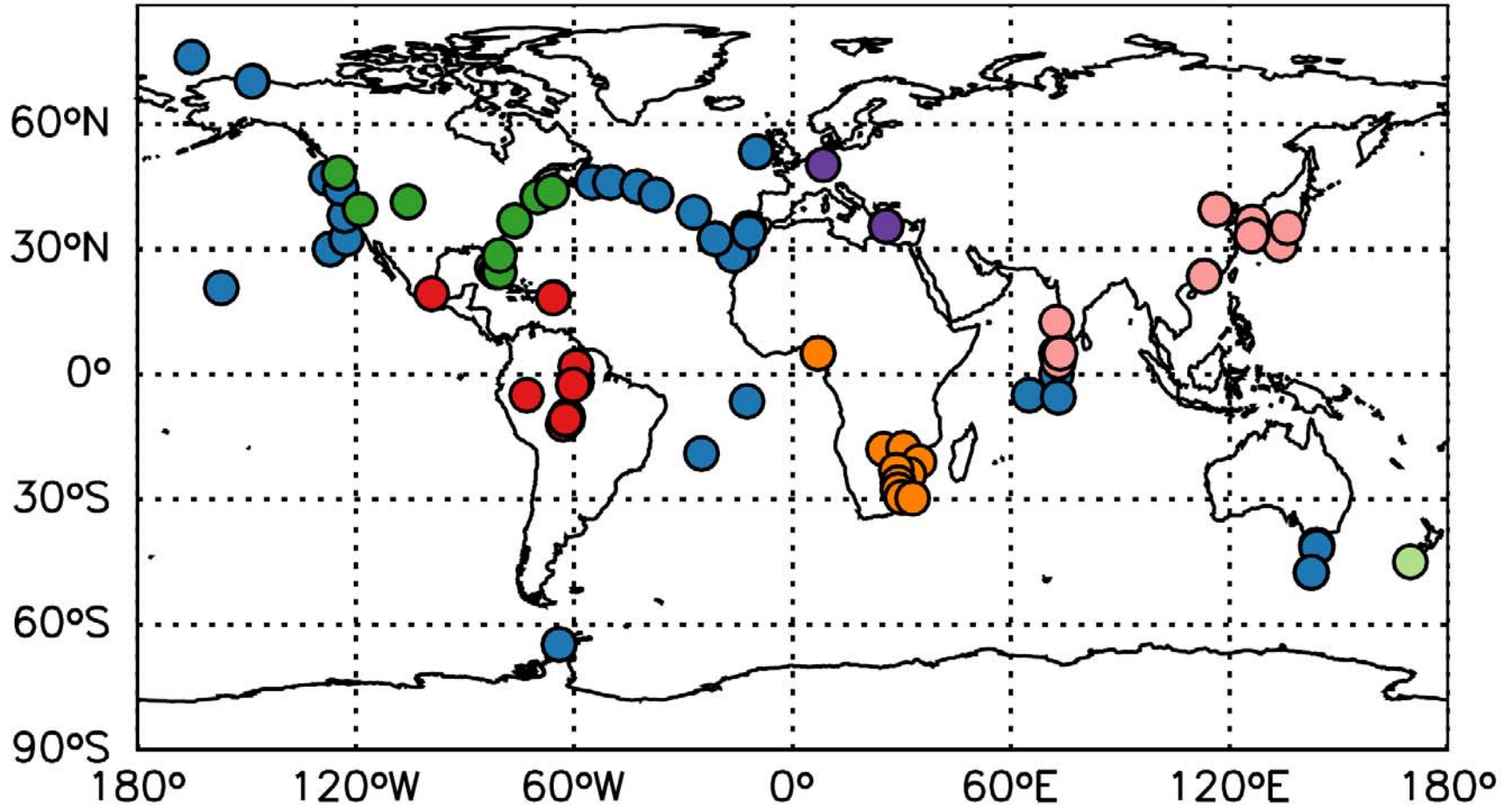
UNIVERSITY OF LEEDS



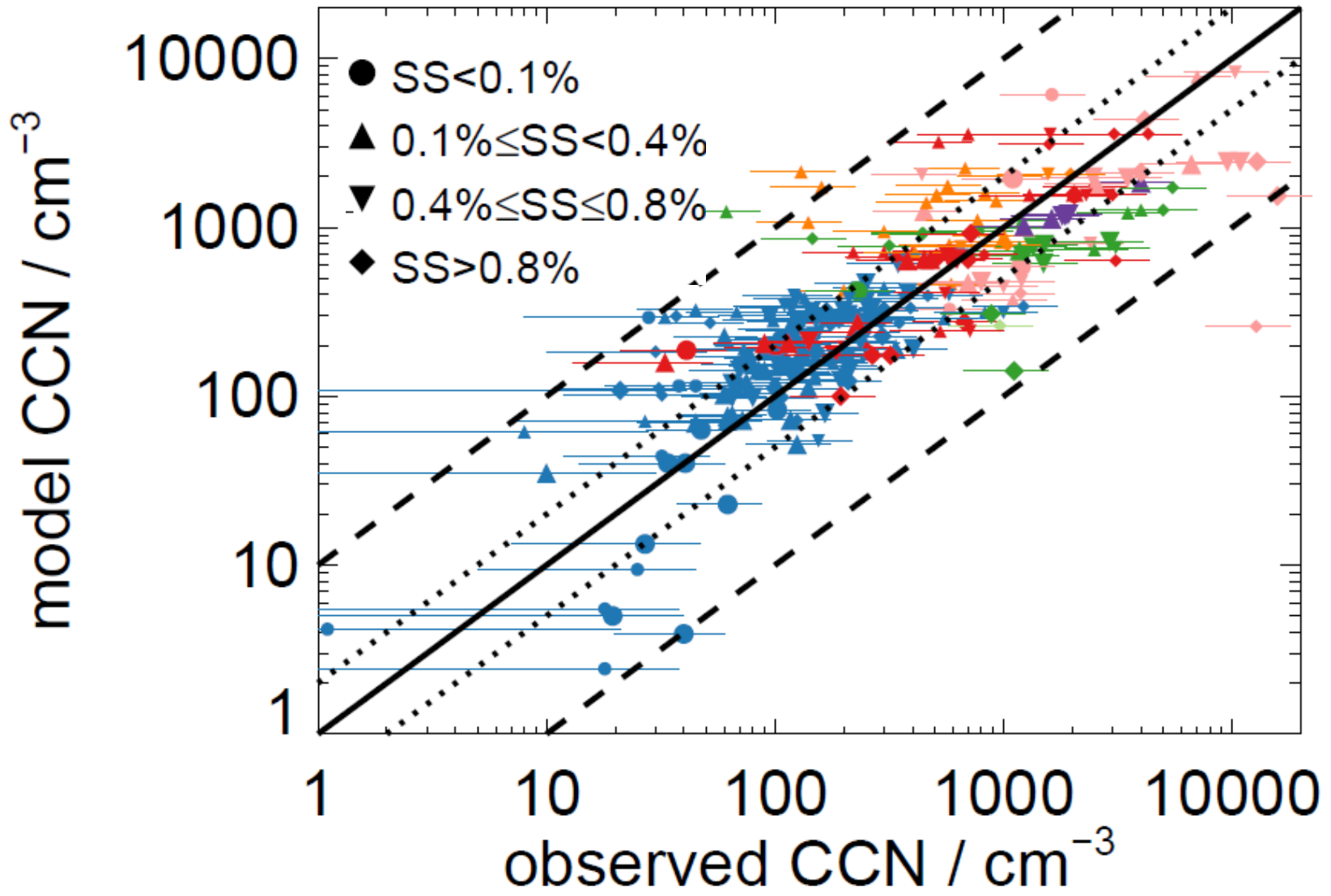
Clarke & Kapustin (2002)



4. Compilation of CCN counter measurements



Compilation of CCN observations gathered by Dominick Spracklen (Leeds) (Spracklen et al, 2011, ACPD)



5. Size distribution at EUSAAR supersites

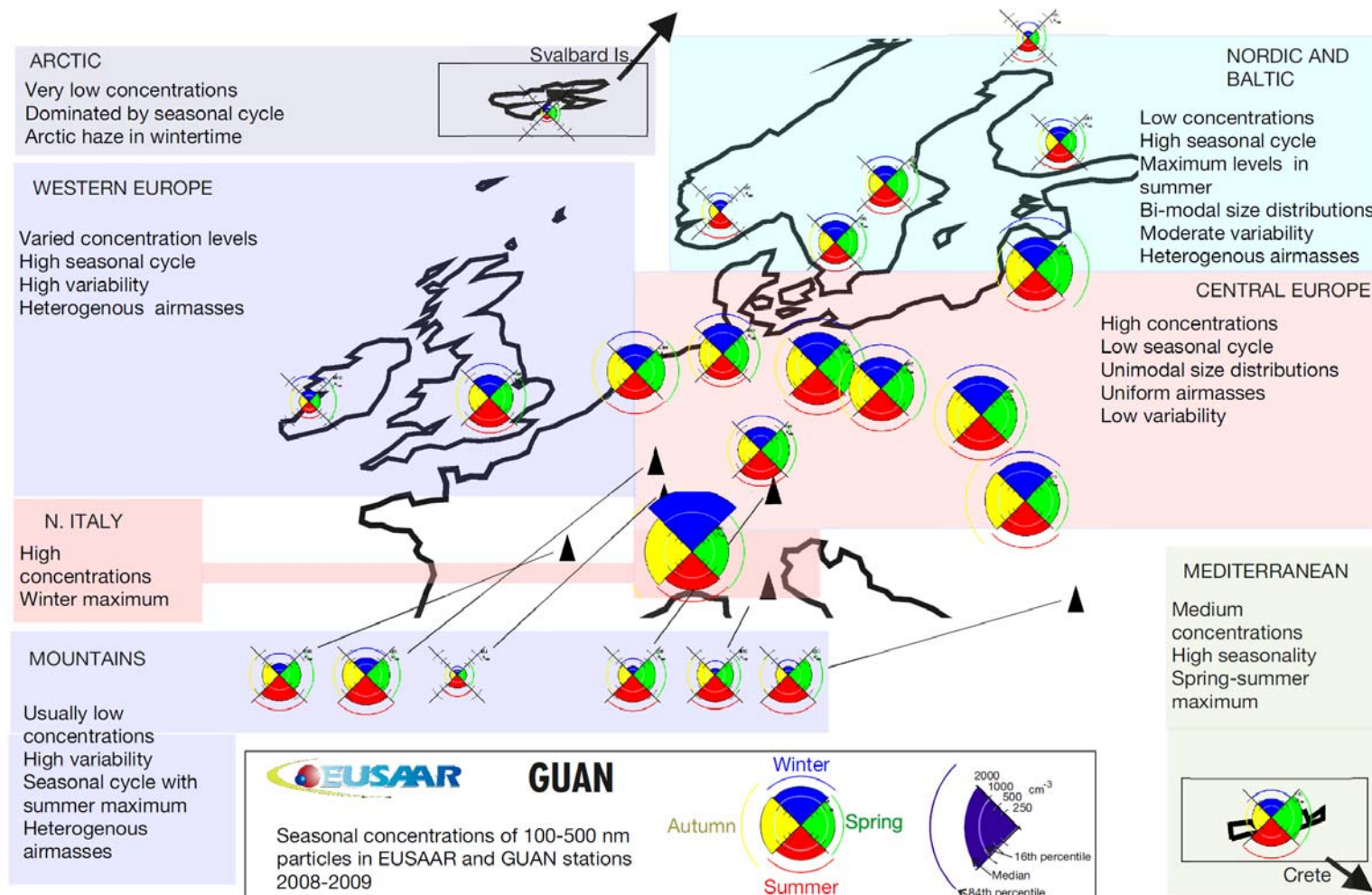
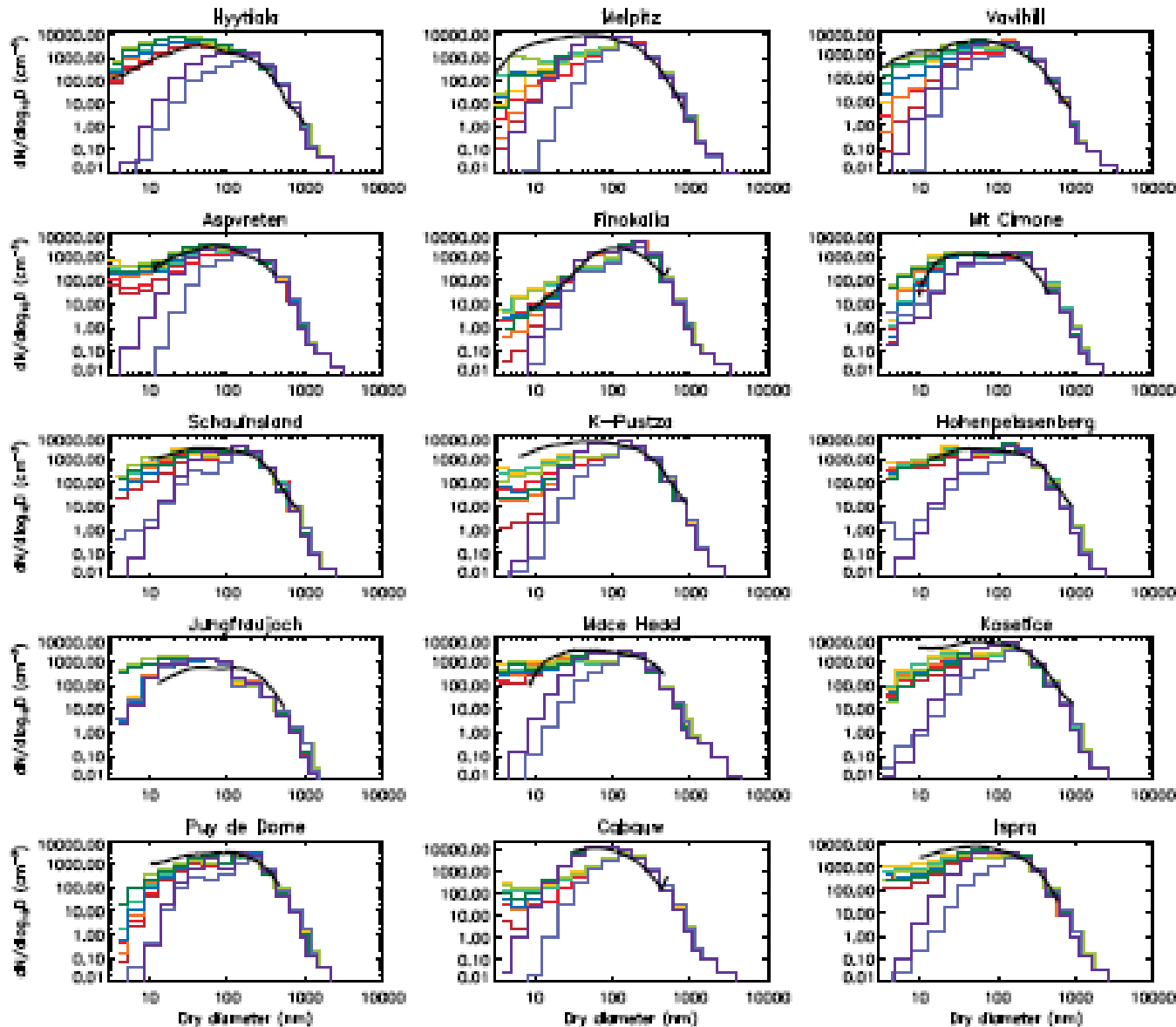


Fig. 15. Overview of EUSAAR and GUAN station measurements – spatial distribution of particle number concentrations on particle (in cm^{-3} STP). The coloured areas are relative to the median concentration observed in each season, and the lower and higher arcs show 16th and 84th percentile concentrations. The colours and location of the segments show different seasons. The locations of the stations are approximate. Stations ZEP (Arctic) and FKL (Mediterranean) are located in inserts.



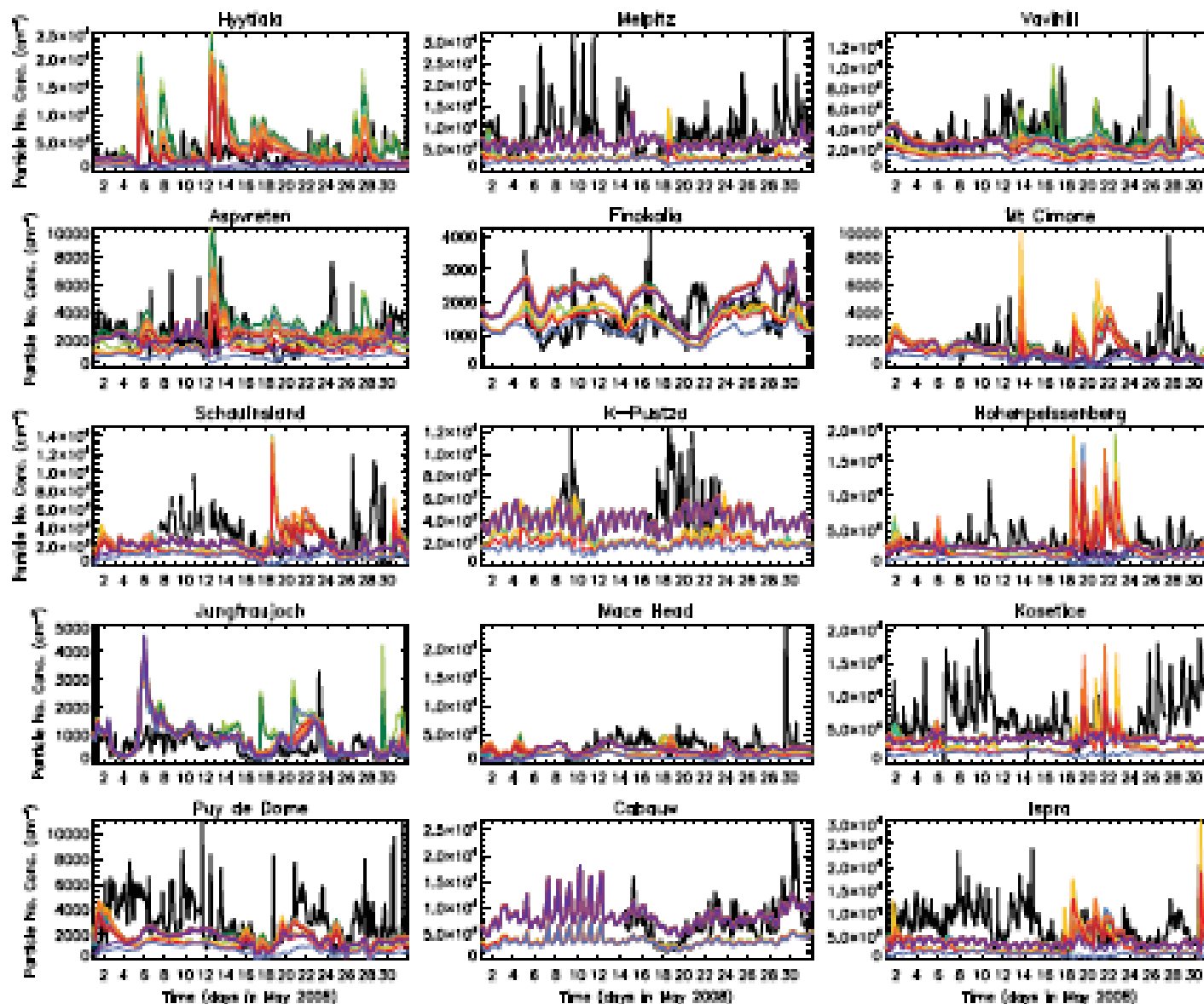
5. Size distribution at EUSAAR supersites



Reddington et al, 2011, ACPD)



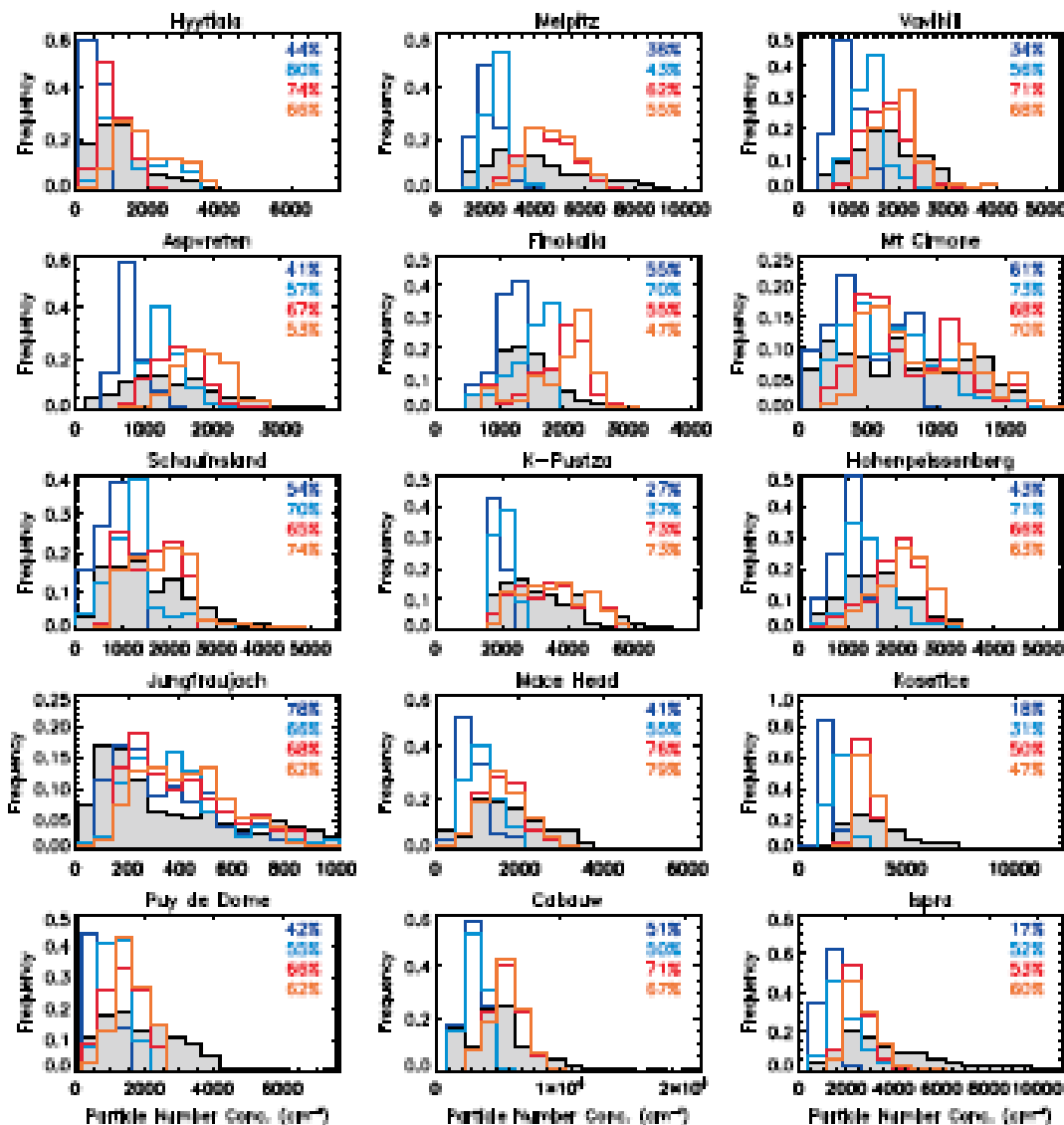
5. Size distribution at EUSAAR supersites



Reddington et al, 2011, ACPD)



5. Size distribution at EUSAAR supersites



Reddington et al, 2011, ACPD)



Influence of microphysics on CN and CCN,

In addition to scoring vs observations, evaluate diversity in simulated influence of primaries/nucleation/coagulation/condensation on simulated CN and CCN

Table 2. Summary of ground level contribution from primary particles (PR), boundary layer nucleation (BLN) and upper tropospheric nucleation (UTN) to ground level total number (CN) and cloud condensation nuclei (CCN) concentrations at 0.2% and 1.0% supersaturations. The marine regions refer to west of North America (NAM), west of South America (SAM), west of North Africa (NAF), west of South Africa (SAF), and East of North-East Asia (NEA) (see Figure 7).

Region	CN		CCN(1.0%)		CCN(0.2%)	
	Tot [cm^{-3}]	PR-UTN-BLN [%]	Tot [cm^{-3}]	PR-UTN-BLN [%]	Tot [cm^{-3}]	PR-UTN-BLN [%]
Total Global	1064	27-25-47	513	49-33-18	314	61-31-8
Total Marine	758	19-33-48	331	41-44-15	204	52-40-9
NAM	596	20-63-18	384	28-63-8	396	36-56-9
SAM	567	14-41-45	273	31-58-11	148	41-53-7
NAF	1003	12-31-57	413	28-52-20	414	36-48-15
SAF	619	23-41-36	345	40-50-10	266	48-45-7
NEA	1423	35-35-30	877	52-35-13	886	62-30-8
Total Continental	1921	36-18-46	1024	57-23-20	625	69-23-7
Europe	2611	47-11-42	1647	63-15-22	932	67-24-10
Africa	1279	50-20-29	900	63-25-12	719	71-24-6
N. America	2600	20-12-69	1079	40-24-36	554	51-32-17
S. America	1713	36-15-49	922	61-25-14	613	71-26-3
N. Asia	1119	22-26-53	554	38-34-28	288	56-31-13
SE Asia	4543	46-14-40	2443	70-15-14	1384	83-13-4
Oceania	1335	21-20-59	778	34-31-36	431	51-38-11



Summary

Large number of global aerosol microphysics models have submitted the all-aerosol-tracer data to the AEROCOM phase-2 experiments.

Enables a ground-breaking intercomparison of simulated size distributions, CN and CCN concentrations amongst the models.

Document the diversity that exists amongst the aerosol microphysics models

Assembled 5 syntheses of in-situ observations from a wider range of field campaigns and monitoring sites that allow the models to be evaluated objectively and quantitatively.

Produce Taylor-diagrams of model skill-scores in terms of normalised-bias and Pearson correlation coefficient for each datasets/metric.

Generate regional CN, CCN concentrations from the models.

Add other observational syntheses to comparison (although plenty already!)?

Analyse the high-temporal-resolution (0D-H) datasets and produce pdf-based comparisons against those at the EUSAAR-GUAN supersites

Quantify multi-model contributions of primary/secondary aerosol to CCN.



1. CN concentrations from GAW and other sites

Station Name	Location	Altitude (m)	Observation period	Min. cutoff diameter (nm)	Reference
Free troposphere					
Jungfraujoch	8.0E , 46.6N	3580	1995-1999, 2003-2007	10	Weingartner et al. (1999)
Puy de Dome	3.0E, 45.8N	1465	2005-2008	3	Venzac et al. (2009)
Nepal C.O.	86.8E, 28.0N	5079	2007-2008	10	Venzac et al. (2008)
Mauna Loa	155.6W, 19.5N	3397	1975-2000	10	Bodhaine (1996)
South Pole	24.8W, 90S	2841	1974-1999	10	
Pico Espejo	71.1W, 8.5N	4775	2007-2009	10	
Mount Washnigton	71.3W, 44.3N	1910	2002-2005	10	
Marine boundary layer					
Mace Head	350.1E, 53.3N	0	2000, 2002-2007	10	O'Dowd et al. (1998)
Neumayer	8.3W, 70.7S	42	1993-2006	10	Weller and Lampert (2008)
Point Barrow	156.6W, 71.3N	11	1994-2007	10	Bodhaine (1989)
Samoa	170.6W, 14.2S	77	1977-2006	10	
Trinidad Head	124.2W, 41.1N	107	2002-2007	10	
Cape Grim	144.7E, 40.6S	94	1996-2007	3	Gras (1995)
Sable Island	60.0W 43.9N	5	1992-2000	10	



1. CN concentrations from GAW and other sites

Station Name	Location	Altitude (m)	Observation period	Min. cutoff diameter (nm)	Reference
Continental boundary later					
Hyytiälä	24.3E, 61.9N	180.	2000-2004	3	Aalto et al. (2001)
Pallas	24.1E, 68.0N	340.	2000-2004, 2007	10	Komppula et al. (2003)
Finokalia	25.7E, 35.3N	0	1997, 2006-2007	10	
Hohenpeissenberg	11.0E, 47.8N	995	2006-2007	3	Birmili et al. (2003)
Melpitz	12.3E, 51.2N	86	1996-1997, 2003	3	
Bondville	88.4W, 40.1N	213	1994-2007	10	
Southern Great Plains	97.5W, 36.6N	320	1996-2007	10	
Tomsk	85.1E, 56.5N		2005-2006	3	Dal Maso et al. (2008b)
Listvyanka	104.9E, 51.9N		2005-2006	3	Dal Maso et al. (2008b)
Harwell	359.0E, 51.0N	60	2000	10	
Weybourne	1.1, 53.0N	0	2005		
Botsalano	25.8E, 25.5S	1424	7/2006-6/2007	10	Laakso et al. (2008)
India Himilaya	79.6E, 29.4N	2180	2005-2008	10	Komppula et al. (2009)
Aspvreten	17.4E, 58.8N	25	2000-2006	10	Dal Maso et al. (2008a)
Utö	21.4E, 59.8N	8	2003-2006	7	Dal Maso et al. (2008a)
Varriö	29.6E, 67.8N	400	1998-2006	8	Dal Maso et al. (2008a)
Thompson Farm	289.1E, 43.1N	75	2001-2009	7	Ziemba et al. (2007)
Castle Springs	71.3W, 43.7N	406	2001-2008	7	

Location	Latitude/Longitude	Time	S (%)	CCN Instrument ¹	Platform ² ; Campaign	Field	Reference
Japan, SW Islands	132–136° E, 30-32° N	16–28 Apr 2001	0.3	TGDCC	A; APEX-E2/ACE-Asia		Adhikari et al., 2005
South Atlantic	40–10° W, 19° S	Feb–Mar 1991	0.3	TGDCC	Sh		Andreae et al., 1995
Cape Grim, Tasmania	144.7° E, 40.7° S	Long term	0.23–1.3		Su		Ayers et al., 1997; Ayers et al., 1991
Mexico City	99.1° W, 19.3° N	13–29 Sep 2000	0.5	STGDCC	Su		Baumgardner et al., 2004
Indian Ocean	60–75° E, 15° S–15° N	Feb-Mar 1998	0.5; 0.75	CCNR	Sh; INDOEX;		Cantrell et al., 2000
Coastal Florida	83–81° W, 24–27° N	Jun–Jul 2002	0.85	CCNS	A; CRYSTAL FACE		Conant et al., 2004; Van Reken et al., 2003
Tanus Observatory, Germany	8.4° E, 50.2° N	20 Jul–11 Aug 2004	0.4	SDC	Su		Dusek et al., 2006
N. Atlantic	75° W–37.5° W, 37–43° N	May 1977	0.16–0.85	TGDCC (0.2–1%), IHC (< 0.2%)	Sh		Hoppel, 1979
N. Atlantic, Tenerife	17.7–10.5° W, 28–32° N	Jun–Jul 1997	0.1	CCNS	A, ACE-2		Chuang et al., 2000
Korea Global Atmospheric Watch	126.3° W, 36.5° N	1–22 May 2004	1.0	DRI	Su		Yum et al., 2005
Arctic, 500 km N of Alaskan coast	165° W, 76° N	May 1998	0.8	DRI	A; Arctic Clouds Experiment		Yum and Hudson, 2001
Southern Africa	22–36.5° E, 15–30.5° S	Aug–Sep 2000; Jan 1999; Mar–Apr 2001	0.3	Wyoming STGDCC	SAFARI-2000; ARREX-1999; ARREX-2001		Ross et al., 2003
Off west coast of US	130–124° W, 38–44° N	Apr 2004	0.2–1.0	Wyoming STGDCC/DMT-CCNC	Sh, CIFEX		Roberts et al., 2006
Mace Head, Ireland	9.9° W, 53.3° N	Mar 1994–Sep 1002	0.5	M-1	Su		Reade et al., 2006
Pacific Ocean off coast of California, USA	125–120° W; 31–34° N	Jun–Jul 1987	0.02-1.0	DRI	A, FIRE-1		Hudson and Xie, 1999; Hudson and Frisbie, 1991b
Atlantic Ocean between Canaries and Azores	25–17.5° W, 27.5–37.5° N	Jun 1992	0.02–0.6	DRI	A, ASTEX		Hudson and Xie, 1999; Yum and Hudson, 2002
Balbina, Amazon basin	59.4° W, 1.92° S	Mar–Apr 1998	0.15–1.5	STGDCC	Su, LBA-CLAIRE		Roberts et al., 2001
Indian Ocean	72–74° E, 8° S–0° S	Feb–Mar 1999	0.1–1.0	DRI	Sh, INDOEX		Hudson and Yum, 2002
Southern Ocean, off Cape Grim, Tasmania	144° E, 43–44° N	Jan–Feb 1995; Jul 1993	0.02–1.0	DRI	SOCEX-I and SOCEX-II		Yum and Hudson (2004)
Pacific Ocean, near Hawaii	156.9° W, 20.7° N	Jul–Aug 1990	0.8	DRI	HaRP		Hudson (1993)
Pacific Ocean, off the coast of Washington State, USA	128° W, 47° N	Dec 1988; June 1989, April 1990	1.0	CCNS	A		Hegg et al., 1991
Reno, USA	119.8° W, 39.5° N	Dec 1988–May 1990	0.75	DRI	Su		Hudson and Frisbie (1991a)
North Atlantic	11–13° W, 32–38° N	Jul 1997	0.2–1.0	CCN spectrometer	A; ACE-2;		Johnson et al. 2000
Puerto Rico	65.6° W, 18.4° N	9–18 Dec 2004	0.5; 0.6	Mainz SDC	Su		Allan et al., 2008

Location	Latitude/Longitude	Time	S (%)	CCN Instrument ¹	Platform ² ; Field Campaign	Reference
Puerto Rico	65.7° W, 18.3° N	29 Mar–9 Apr 1992	0.5	M-1	Su	Novakov and Penner, 1993
Rondonia, Amazon Basin	61.9° W, 10.9° S	Jan–Mar 1999, Oct–Nov 1999	1.0	M-1	LBA-EUSTACH	Williams et al. 2002
Amazon Basin	73° W, –5° N & 63° W, 12° S	Oct 2002	1.0	STGDCC	LBA-SMOCC	Andreae et al., 2004
Atlantic Ocean	11–14° W, 33–40° N	Jul 1997	0.2	CCNS	A; ACE-2	Osborne et al., 2000
Atlantic Ocean	11–13° W, 30–38° N	Jul 1997	0.2–1.0	CCN Spectrometer	A; ACE-2	Wood et al., 2000
NW Korea	126.2° W, 33.3° N	Mar–Apr 2005	0.6	DMT-CCNC	Su	Yum et al., 2007
Nagoya, Japan	135.9° E, 35.1° N	Dec 1998–Jan 1999	0.5	CCNC	Su	Ishizaka et al., 2003
Palmer station, Antarctica	64.1° W, 64.8° S	Jan–Feb 1994	1.0; 0.3	CCNS	Su	Defelice et al., 1997
Finokalia, Greece	25.7° E, 35.5° N	Jun–Oct 2007	0.21–0.73	DMT-CCNC	Su	Bougiatioti et al., 2009
East coast of Florida, USA	80.5° W, 28.5° N	Jul–Aug 1995	1.0	DRI	A; SCMS	Hudson and Yum, 2001
Jeju Island, Korea	126.1° E, 33.2° N	Mar–Apr 2005	0.09-0.97	DMT-CCNC	Su, Atmospheric Brown Cloud	Kuwata et al., 2008
Kaashidhoo Climate Observatory	73.47° E, 4.97° N	Feb–Mar 1999	0.3, 0.5	CCNR	Su, INDOEX;	Cantrell et al., 2001
Laramie, Wyoming, USA	105.6° W, 41.3° N	Jun–Sep 1996; Nov 1995; Jan 1997	1.0	STGDCC	A	Delene and Deshler, 2001
Lauder, New Zealand	169.7° E, 45.0° S	Feb 1996	1.0	STGDCC	A	Delene and Deshler, 2001
Ivory Coast, Africa	7° E, 5° N	Dry & wet season	0.32-0.85	TGDCC	Su	Désalmand, 1985
Tenerife, Atlantic	16.3° W, 28.5° N	Jun–Jul 1997	1.0	Wyoming STGDCC	A; ACE-2	Snider and Brenguier, 2000
Arctic, Near Prudhoe Bay, Alaska	70.3° N, 148.3° W	Jun 1995	1.0	CFDCC	A	Hegg et al., 1996
NW Atlantic, off Nova Scotia	43.8° N, 66.1° W	Aug–Sep 1993	0.06; 0.4	M1 (0.4%); IHC(0.06%)	A, NARE	Liu et al., 1996
El Yunque peak, Puerto Rico	65.75° W, 18.32° N	Mar–Apr 1992	0.5	M1	Su	Rivera-Carpio et al., 1996
Point Reyes, California coast, USA	122.98° W, 38° N	Oct 1993, Jun–Jul 1994	0.5	M1	Su	Rivera-Carpio et al., 1996
Amazon basin	59.5° W, 1.9° S	Jul 2001	0.12–1.2	STGDCC	Su	Rissler et al., 2004
Oregon Coast, USA	124.1° W, 44.6° N	Jan and Jul 1971	0.1–1.0	TGDCC	Sh	Elliot and Egami, 1975
Southern Ocean, near Tasmania	137°–160° E, 40°–55° S	Nov–Dec 1995	0.02-1.0	DRI	A, ACE-1	Hudson et al., 1998
Arctic Ocean, near Deadhorse, Alaska	148.5° W, 70.2° N	Apr 1992	1.0	CCNS	A, DEADEX	Hegg et al., 1995
Amazon Basin, near Manaus, Brazil	60.21° W, 2.59° S	Feb–Mar 2008	0.1–0.82	DMT-CCNC	Su; AMAZE	Gunthe et al., 2009
Fallon, Nevada, USA	118.78° W, 39.47° N	Aug–Oct 1975	0.91	CFDCC	Su	Hudson and Squires, 1978



Location	Latitude/Longitude	Time	S (%)	CCN Instrument ¹	Platform ² ; Campaign	Field	Reference
Cheeka Peak, Washington State, USA	124.62° W, 48.3° N	Apr 1991	0.3	STGDCC	Su		Quinn et al., 1993
NE Atlantic Ocean	27.1° W, 38.8° N	Jun 1992	1.0	CCNS	A		Hegg et al., 1993
Fazenda Nossa, Amazon basin	62.35° W, 10.8° S	Oct to Nov 2002	0.2–1.12	TGDCC	Su, LBA-SMOCC		Vestin et al., 2007
Guangzhou, China	113.1° E, 23.54° N	1–30 Jul 2006	0.07-1.27	DMT-CCNC	Su		Rose et al., 2010

¹ DRI: Desert Research Institute (DRI) airborne instantaneous CCN spectrometer (Hudson, 1989); CCN spectrometer (Hoppel et al., 1979; Saxena and Kassner, 1970; Fukuta and Saxena, 1979a, b; Radke et al., 1981); DMT-CCNC: Droplet measurement technologies (DMT) stream-wise thermal-gradient CCN counter (Roberts and Nenes, 2005; Lance et al., 2006; Rose et al., 2008); CCNR: CCN Remover (Ji et al., 1998); TGDCC: Thermal-gradient diffusion cloud chamber (Désalmand, 1985); STGDCC: Static thermal-gradient diffusion cloud chamber (Delene et al., 1998; Delene and Deshler, 2000); IHC: Isothermal Haze Counter (Fitzgerald et al., 1981); M-1: DH Associates, parallel-plate diffusion cloud chamber (Phillipin and Betterton, 1997); SDC: Static parallel-plate thermal-gradient diffusion cloud chamber (Frank et al., 2007); CFDC: Continuous-flow diffusion cloud chamber (Hudson and Squires, 1976; Hudson and Alofs, 1981); CCNC: CCN counter (Model 130, Mee) (Ishizaka et al., 2003).

² Su: surface; Sh: ship; A: above the surface (aircraft or balloon).



Development of process-based global aerosol microphysics models



Process models can include high complexity

In box models, 2D models or 3D offline models of short integrations, one can afford to track high degree of sophistication

160 tracers for a basic fully internally mixed size and composition resolved distribution

~260 tracers to resolve basic 'fresh' particles

>400 tracers to resolve ageing of fresh particles

But in a climate model (e.g. HadGEM):
25 tracers for aerosol considered high

dust

OC

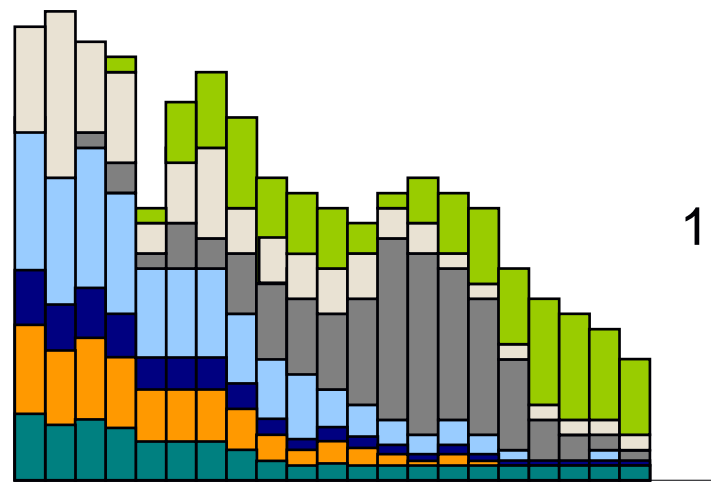
BC

SO₄²⁻

NO₃⁻

NH₄⁺

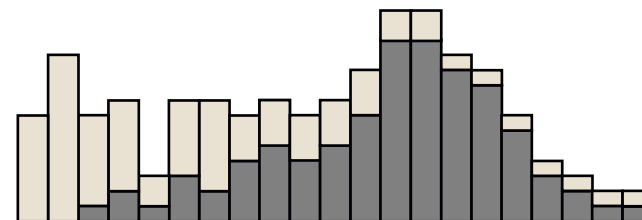
Na⁺



160 tracers

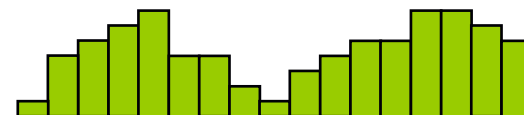
OC

BC



60 tracers

dust

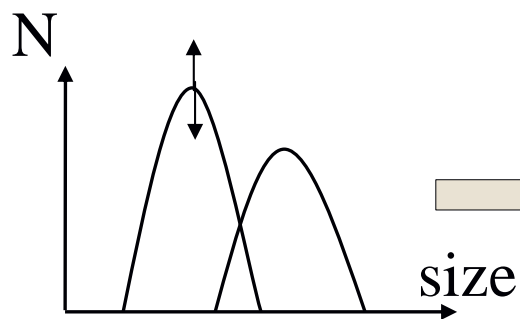


40 tracers

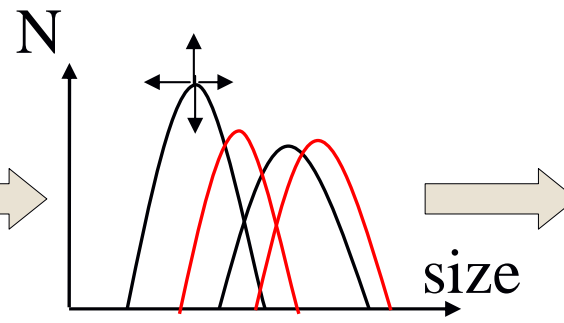
Evolution of complexity in aerosol-climate models

Current state-of-the-science in aerosol-climate models has moved on from 1st generation mass-based only models.

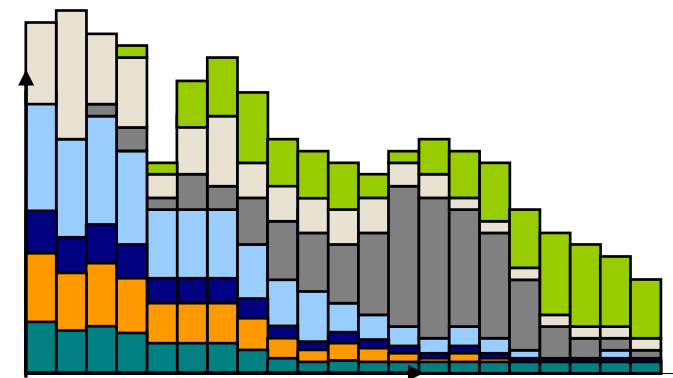
Established recognition now that aerosol-climate models need to simulate particle number to allow size distribution to evolve according to the chemical & microphysical processes, and represent of size-resolved chemical composition



*1st generation
climate model
schemes*



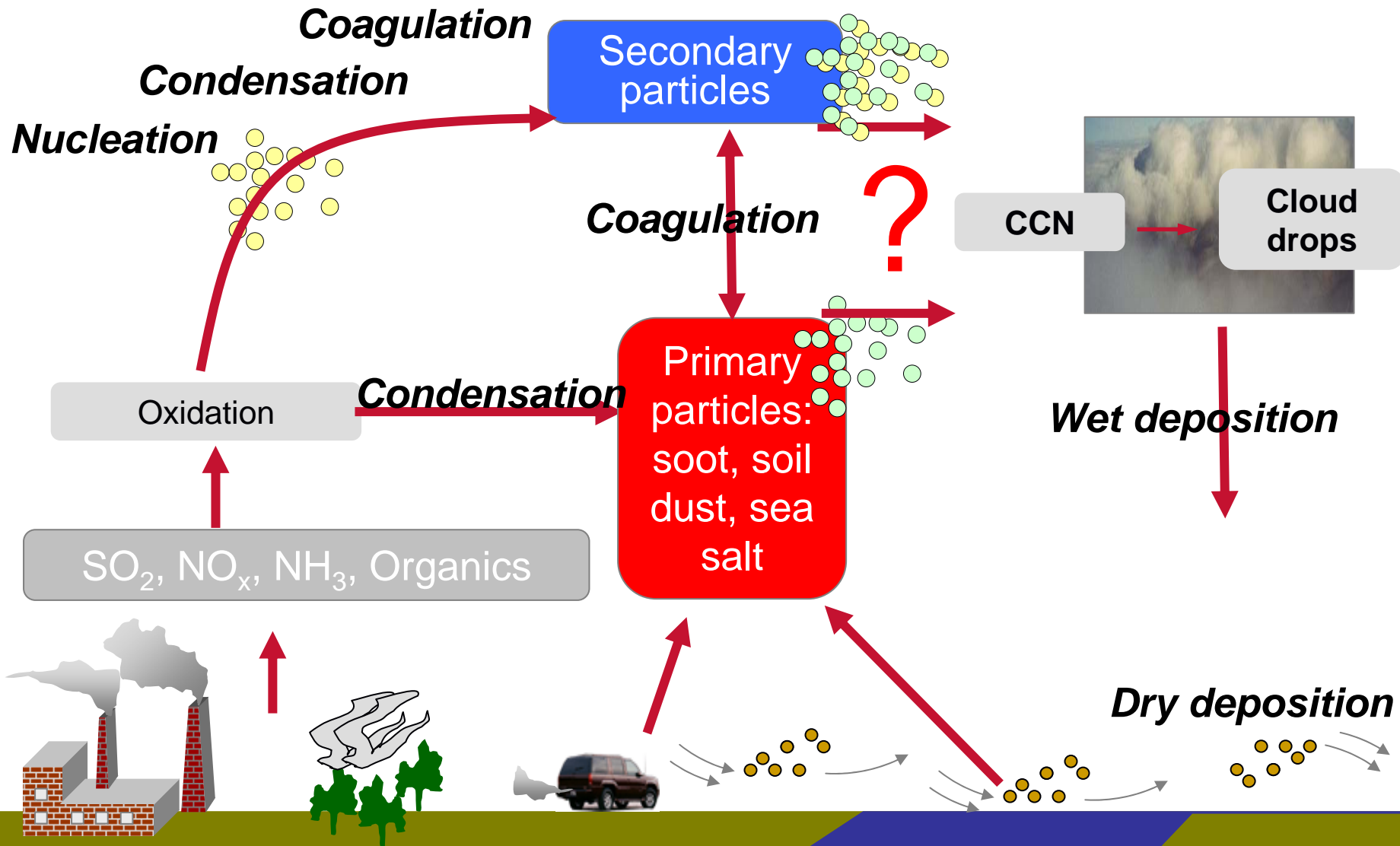
*New generation of
climate models with
modal aerosol dynamics*



*“Research models”
bin-resolved
Future GCMs?*



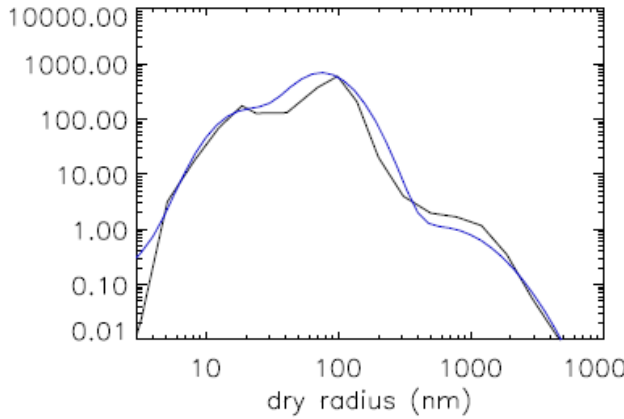
Primary & secondary sources of aerosol



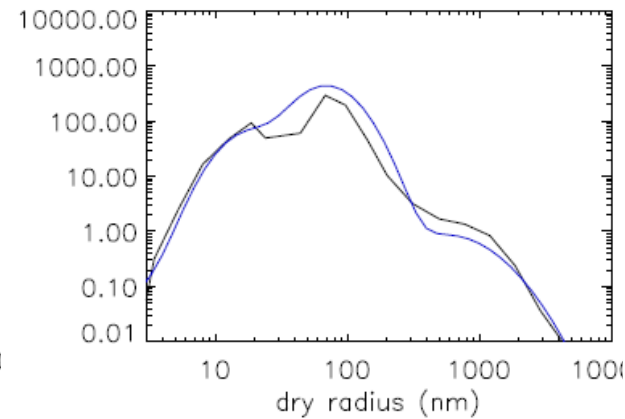


Benchmark GLOMAP-mode vs bin in CTM

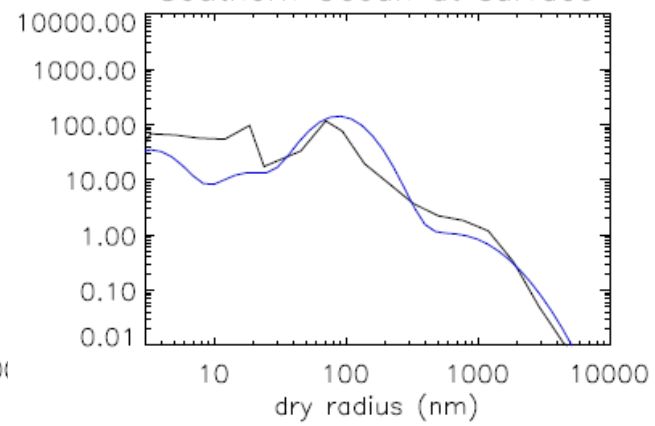
Atlantic at surface



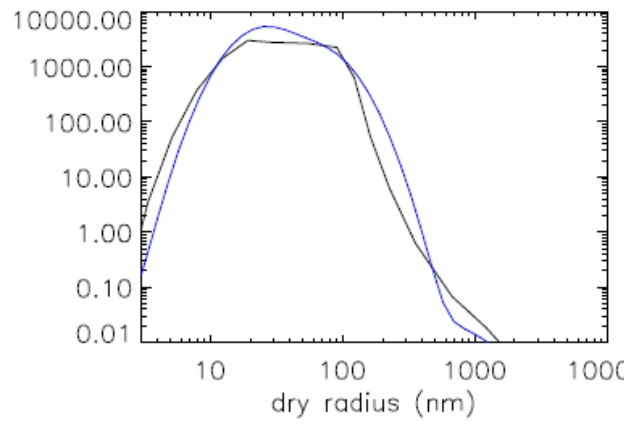
N. Pacific at surface



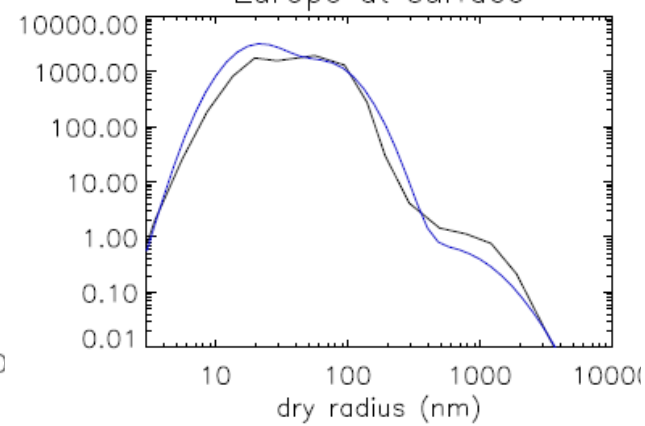
Southern Ocean at surface



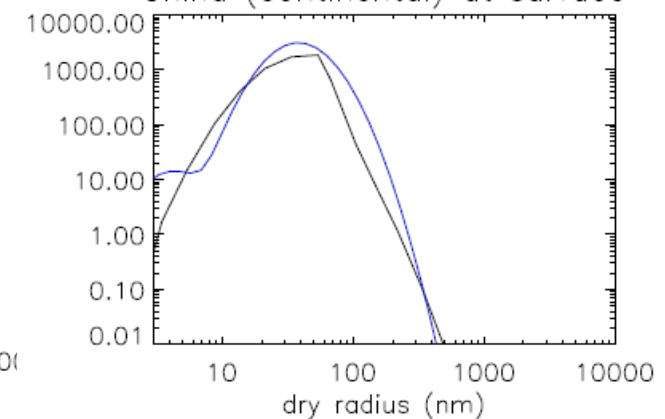
E. USA at surface



Europe at surface



China (continental) at surface



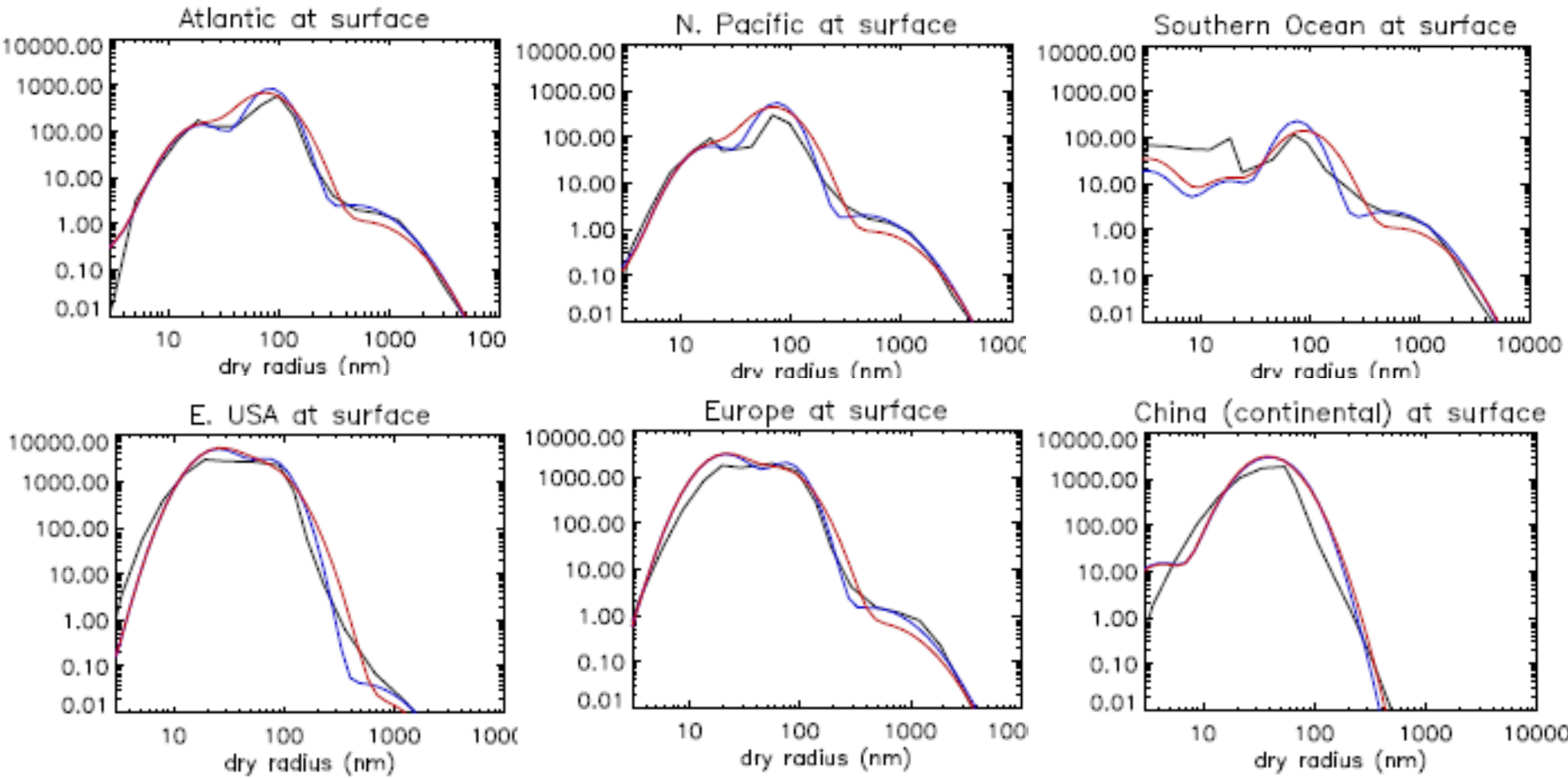
GLOMAP-bin

GLOMAP-mode ($\sigma\text{-acc}=1.59$, $d\text{plim}34=1000\text{nm}$ as M7)

Mann et al, in prep, 2011



Improve GLOMAP-mode vs bin in CTM



Mann et al, in prep, 2011

GLOMAP-bin

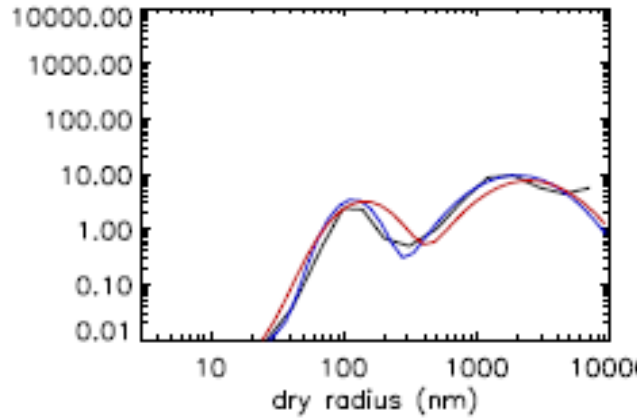
GLOMAP-mode (sigma-acc=1.59, dplim34=1000nm as M7)

GLOMAP-mode (sigma-acc=1.40, dplim34= 500nm)

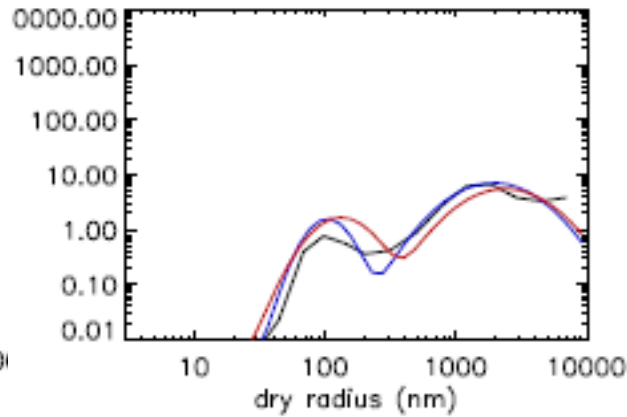


Improve GLOMAP-mode vs bin in CTM

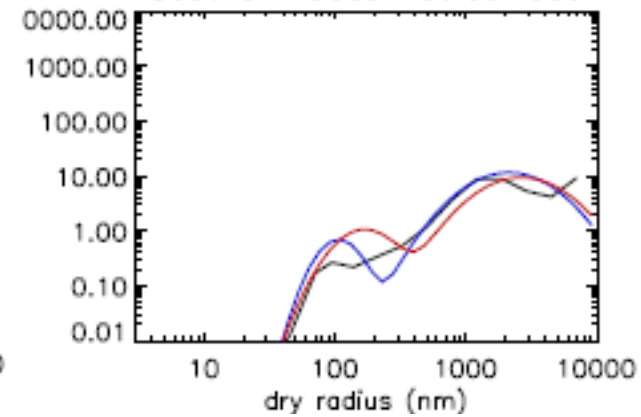
Atlantic at surface



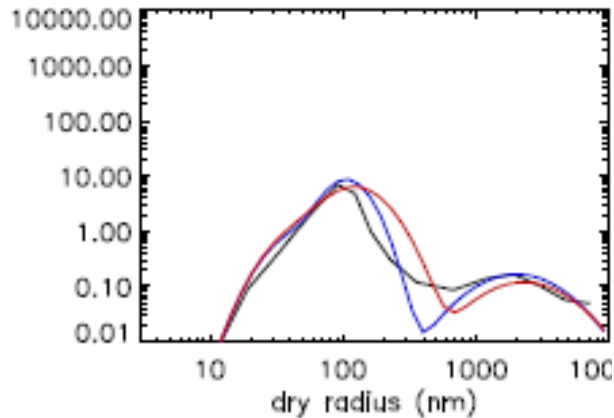
N. Pacific at surface



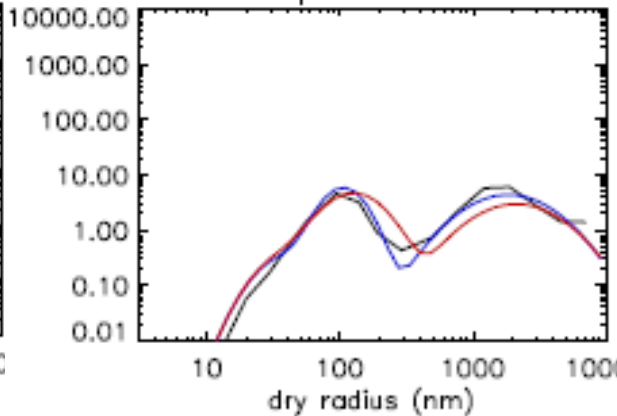
Southern Ocean at surface



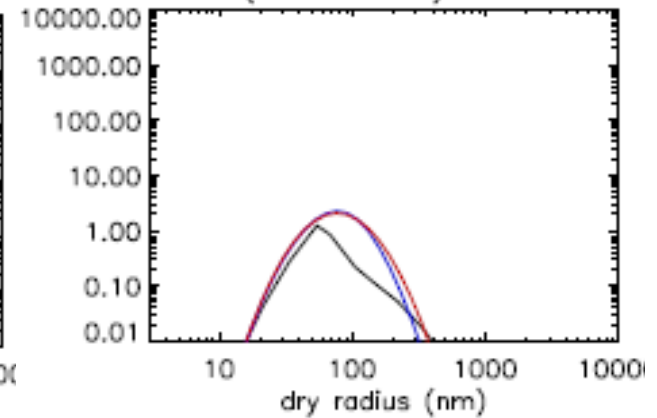
E. USA at surface



Europe at surface



China (continental) at surface



GLOMAP-bin

Mann et al, in prep, 2011

GLOMAP-mode (sigma-acc=1.59, dplim34=1000nm as M7)

GLOMAP-mode (sigma-acc=1.40, dplim34= 500nm)

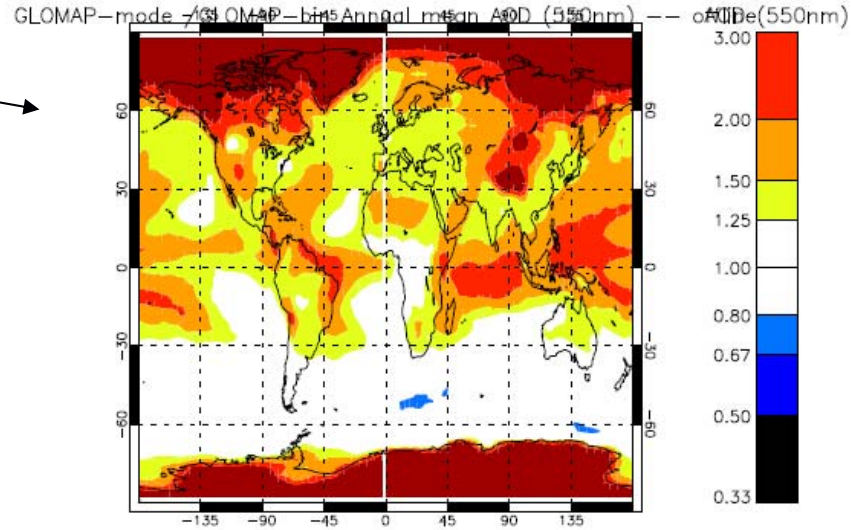


Improve GLOMAP-mode vs bin in CTM

Original model

AOD high-bias greatly reduced due following examination of size-distbns

Revised model



Mann et al, in prep, 2011

